

Chapter 5. Some Exactly Solvable Problems

The objective of this chapter is to describe several relatively simple but important applications of the bra-ket formalism, including a few core problems of wave mechanics we have already started to discuss in Chapters 2 and 3.

5.1. Two-level systems

The discussion of the bra-ket formalism in the previous chapter was peppered with numerous illustrations of its main concepts on the examples of “spin- $\frac{1}{2}$ -like” systems with the smallest non-trivial (two-dimensional) Hilbert space. In such a system, the bra- and ket-vectors of an arbitrary quantum state α may be represented as a linear superposition of just two basis vectors, for example

$$|\alpha\rangle = \alpha_{\uparrow}|\uparrow\rangle + \alpha_{\downarrow}|\downarrow\rangle, \quad (5.1)$$

where the states \uparrow and \downarrow are defined as the eigenstates of the Pauli matrix σ_z – see Eq. (4.105). For the genuine spin- $\frac{1}{2}$ particles (such as electrons) placed in a z -oriented time-independent magnetic field, these states are the stationary “spin-up” and “spin-down” stationary states of the Pauli Hamiltonian (4.163), with the corresponding two energy levels (4.167).

However, an approximate but reasonable quantum description of some other important systems may also be given in such Hilbert space. For example, as was discussed in Sec. 2.6, two weakly coupled space-localized orbital states of a spin-free particle are sufficient for an approximate description of its quantum oscillations between two potential wells. A similar coupling of two traveling waves explains the energy band splitting in the weak-potential approximation of the band theory – Sec. 2.7. As will be shown in the next chapter, in systems with time-independent Hamiltonians, such a situation almost unavoidably appears each time when two energy levels are much closer to each other than to other levels. Moreover, as will be shown in Sec. 6.5, a similar truncated description is adequate even in cases when two levels E_n and $E_{n'}$ of an unperturbed system are not close to each other, but the corresponding states become coupled by an applied ac field of a frequency ω very close to the difference $(E_n - E_{n'})/\hbar$. Such *two-level systems* are nowadays the focus of additional attention in the view of prospects of their use for quantum information processing and encryption.¹ This is why I will spend a bit more time reviewing the main properties of an arbitrary two-level system.

The most general form of the Hamiltonian of a two-level system is represented, in an arbitrary basis, by a 2×2 matrix

$$H = \begin{pmatrix} H_{11} & H_{12} \\ H_{21} & H_{22} \end{pmatrix}. \quad (5.2)$$

According to the discussion in Secs. 4.3-4.5, since the Hamiltonian operator has to be Hermitian, the diagonal elements of the matrix H have to be real, and its off-diagonal elements have to be complex

¹ In the last context, to be discussed in Sec. 8.5, the two-level systems are usually called *qubits*.

conjugate: $H_{21} = H_{12}^*$. As a result, we may not only represent H as a linear combination (4.106) of the identity matrix and the Pauli matrices but also reduce it to a more specific form:

$$H = bI + \mathbf{c} \cdot \boldsymbol{\sigma} = \begin{pmatrix} b + c_z & c_x - ic_y \\ c_x + ic_y & b - c_z \end{pmatrix} \equiv \begin{pmatrix} b + c_z & c_- \\ c_+ & b - c_z \end{pmatrix}, \quad \text{with } c_{\pm} \equiv c_x \pm ic_y, \quad (5.3)$$

where the scalar b and the Cartesian components of the vector \mathbf{c} are *real* c -number coefficients:

$$b = \frac{H_{11} + H_{22}}{2}, \quad c_x = \frac{H_{12} + H_{21}}{2} \equiv \text{Re } H_{21}, \quad c_y = \frac{H_{21} - H_{12}}{2i} \equiv \text{Im } H_{21}, \quad c_z = \frac{H_{11} - H_{22}}{2}. \quad (5.4)$$

If such a Hamiltonian does not depend on time, the corresponding characteristic equation (4.103) for the system's energy levels E_{\pm} ,

$$\begin{vmatrix} b + c_z - E & c_- \\ c_+ & b - c_z - E \end{vmatrix} = 0, \quad (5.5)$$

is a simple quadratic equation, with the following roots:

$$E_{\pm} = b \pm c \equiv b \pm (c_+ c_- + c_z^2)^{1/2} \equiv b \pm (c_x^2 + c_y^2 + c_z^2)^{1/2} \equiv \frac{H_{11} + H_{22}}{2} \pm \left[\left(\frac{H_{11} - H_{22}}{2} \right)^2 + |H_{21}|^2 \right]^{1/2}. \quad (5.6)$$

The parameter $b \equiv (H_{11} + H_{22})/2$ evidently gives the average energy $E^{(0)}$ of the system, which does not contribute to the level splitting

$$\Delta E \equiv E_+ - E_- = 2c \equiv 2(c_x^2 + c_y^2 + c_z^2)^{1/2} \equiv \left[(H_{11} - H_{22})^2 + 4|H_{21}|^2 \right]^{1/2}. \quad (5.7)$$

So, the splitting is a hyperbolic function of the coefficient $c_z \equiv (H_{11} - H_{22})/2$. A plot of this function is the famous level-anticrossing diagram (Fig. 1), which has already been discussed in Sec. 2.7 in the particular context of the weak-potential limit of the 1D band theory.

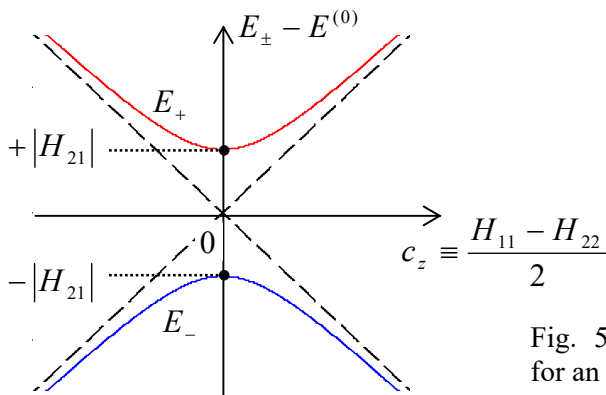


Fig. 5.1. The level-anticrossing diagram for an arbitrary two-level system.

The physics of the diagram becomes especially clear if the two states of the basis used to spell out the matrix (2) may be interpreted as the stationary states of two potentially independent subsystems, with the energies, respectively, H_{11} and H_{22} . (For example, in the case of two weakly coupled potential wells discussed in Sec. 2.6, these are the ground-state energies of two very distant wells.) Then the off-diagonal elements $c_- \equiv H_{12}$ and $c_+ \equiv H_{21} = H_{12}^*$ describe the subsystem coupling, and the anticrossing

diagram shows how do the eigenenergies of the coupled system depend (at fixed coupling) on the difference of the subsystem energies. As was already discussed in Sec. 2.7, the most striking feature of the diagram is that any non-zero coupling $|c_{\pm}| \equiv (c_x^2 + c_y^2)^{1/2}$ changes the topology of the eigenstate energies, creating a gap of the width ΔE .

As it follows from our discussions of particular two-level systems in Secs. 2.6 and 4.6, the dynamics of such systems also has a general feature – the quantum oscillations. Namely, if we put any two-level system into any initial state different from one of its eigenstates \pm , and then let it evolve on its own, the probability of its finding the system in any of the “partial” states exhibits oscillations with the frequency

$$\Omega = \frac{2c}{\hbar} = \frac{\Delta E}{\hbar} \equiv \frac{E_+ - E_-}{\hbar}, \quad (5.8)$$

lowest at the exact subsystem symmetry ($c_z = 0$, i.e. $H_{11} = H_{22}$), when it is proportional to the coupling strength: $\Omega_{\min} = 2|c_{\pm}|/\hbar \equiv 2|H_{12}|/\hbar = 2|H_{21}|/\hbar$.

In the case discussed in Sec. 2.6, these are the oscillations of a particle between the two coupled potential wells (or rather of the probabilities to find it in either well) – see, e.g., Eqs. (2.181). On the other hand, for a spin- $\frac{1}{2}$ particle in an external magnetic field, these oscillations take the form of spin precession in the plane normal to the field, with periodic oscillations of its Cartesian components (or rather their expectation values) – see, e.g., Eqs. (4.173)-(4.174). Some other examples of the quantum oscillations in two-level systems may be rather unexpected; for example, the ammonium molecule NH_3 (Fig. 2) has two similar states that differ only by the inversion of the nitrogen atom relative to the common plane of the three hydrogen atoms. These states are weakly coupled due to the quantum-mechanical tunneling of the nitrogen atom through this plane.² Since for this particular molecule, in the absence of external fields, the level splitting ΔE corresponds to an experimentally convenient frequency $\Omega/2\pi \approx 24$ GHz, it played an important historic role in the initial development of the atomic frequency standards and microwave quantum generators (*masers*) in the early 1950s,³ which paved the way for laser technology.

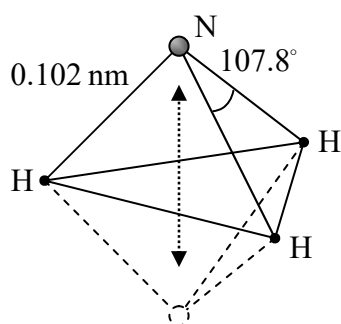


Fig. 5.2. An ammonia molecule and its inversion.

Now let us now discuss a very convenient geometric representation of an arbitrary quantum state α of any two-level system. As Eq. (1) shows, such a state is completely described by two complex

² Since the hydrogen atoms are much lighter, it may be fairer to speak about the tunneling of their triangle around the (nearly immobile) nitrogen atom.

³ In particular, these molecules were used in the demonstration of the first maser by C. Townes' group in 1954.

coefficients (*c*-numbers) – say, α_\uparrow and α_\downarrow . If the vectors of the basis states \uparrow and \downarrow are normalized, then these coefficients must obey the following restriction:

$$W_\Sigma = \langle \alpha | \alpha \rangle = \left(\langle \uparrow | \alpha_\uparrow^* + \langle \downarrow | \alpha_\downarrow^* \right) \left(\alpha_\uparrow | \uparrow \rangle + \alpha_\downarrow | \downarrow \rangle \right) = \alpha_\uparrow^* \alpha_\uparrow + \alpha_\downarrow^* \alpha_\downarrow = |\alpha_\uparrow|^2 + |\alpha_\downarrow|^2 = 1. \quad (5.9)$$

This requirement is automatically satisfied if we take the moduli of α_\uparrow and α_\downarrow equal to the sine and cosine of the same real angle. Thus we may write, for example,

$$\alpha_\uparrow = \cos \frac{\theta}{2} e^{i\gamma}, \quad \alpha_\downarrow = \sin \frac{\theta}{2} e^{i(\gamma+\varphi)}. \quad (5.10)$$

Moreover, according to the general Eq. (4.125), if we deal with just one two-level system,⁴ the common phase factor $\exp\{i\gamma\}$ drops out of the calculation of any expectation value, so we may take $\gamma=0$, and Eq. (10) is reduced to

$$\alpha_\uparrow = \cos \frac{\theta}{2}, \quad \alpha_\downarrow = \sin \frac{\theta}{2} e^{i\varphi}. \quad (5.11)$$

Bloch sphere representation

The reason why the argument of these sine and cosine functions is usually taken in the form $\theta/2$, is clear from Fig. 3a: Eq. (11) conveniently maps each state α of a two-level system onto a certain *representation point* on a unit-radius *Bloch sphere*,⁵ with the polar angle θ and the azimuthal angle φ .

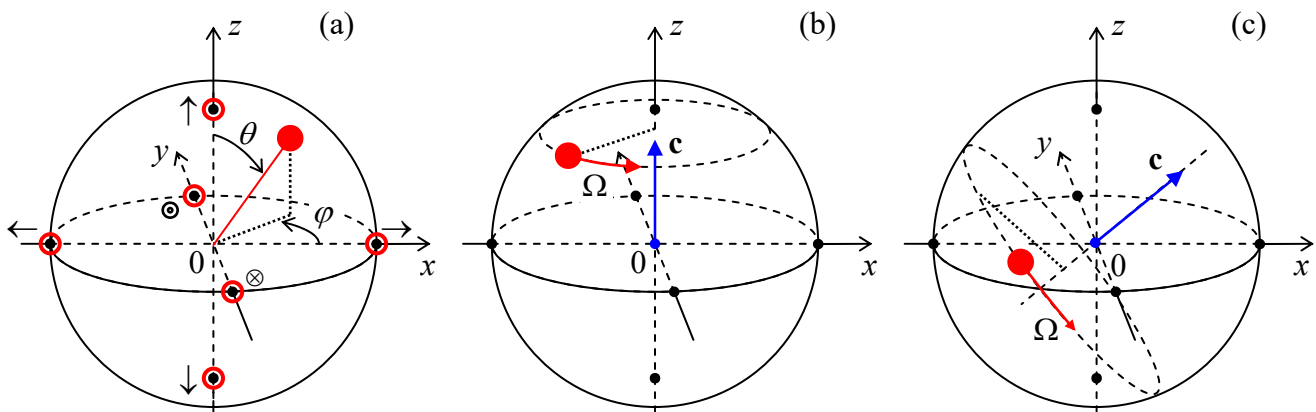


Fig. 5.3. The Bloch sphere: (a) the representation of an arbitrary state (solid red point) and the eigenstates of the Pauli matrices (black-dotted points), and (b, c) the two-level system’s evolution: (b) in a constant “field” \mathbf{c} directed along the z -axis, and (c) in an arbitrarily orientated field.

In particular, the basis state \uparrow , described by Eq. (1) with $\alpha_\uparrow = 1$ and $\alpha_\downarrow = 0$, corresponds to the North Pole of the sphere ($\theta=0$), while the opposite state \downarrow , with $\alpha_\uparrow = 0$ and $\alpha_\downarrow = 1$, to its South Pole ($\theta = \pi$). Similarly, the eigenstates \rightarrow and \leftarrow of the matrix σ_x , described by Eqs. (4.122), i.e. having $\alpha_\uparrow =$

⁴ If you need a reminder of why this condition is crucial, please revisit the discussion at the end of Sec. 1.6. Note also that the mutual phase shifts between different two-level systems are important, in particular, for quantum information processing (see Sec. 8.5 below), so most discussions of these applications have to start from Eq. (10) rather than Eq. (11).

⁵ This representation was suggested in 1946 by the same Felix Bloch who pioneered the energy band theory discussed in Chapters 2-3.

$1/\sqrt{2}$ and $\alpha_{\downarrow} = \pm 1/\sqrt{2}$, correspond to the equator ($\theta = \pi/2$) points with, respectively, $\varphi = 0$ and $\varphi = \pi$. Two more special points (denoted in Fig. 3a as \odot and \otimes) are also located on the sphere's equator, at $\theta = \pi/2$ and $\varphi = \pm\pi/2$; it is easy to check that they correspond to the eigenstates of the matrix σ_y (in the same z -basis).

To understand why this mutually perpendicular location of these three special point pairs on the Bloch sphere is not occasional, let us plug Eqs. (11) into Eqs. (4.131)-(4.133) for the expectation values of the spin- $1/2$ components. In terms of the Pauli vector operator (4.117), $\hat{\sigma} \equiv \hat{\mathbf{S}}/(\hbar/2)$, the result is

$$\langle \sigma_x \rangle = \sin \theta \cos \varphi, \quad \langle \sigma_y \rangle = \sin \theta \sin \varphi, \quad \langle \sigma_z \rangle = \cos \theta, \quad (5.12)$$

showing that the radius vector of any representation point is just the expectation value $\langle \sigma \rangle$.

Now let us use Eq. (3) to see how the representation point moves in various cases, ignoring the term bI – which, again, describes the offset of the total energy of the system relative to some reference level, and does not affect its dynamics. First of all, according to Eq. (4.158), if $\mathbf{c} = 0$ (when the Hamiltonian operator turns to zero, and hence the state vectors do not depend on time) the point does not move at all, and its position is determined by initial conditions, i.e. by the system's preparation. If $\mathbf{c} \neq 0$, we may re-use some results of Sec. 4.6, obtained for the Pauli Hamiltonian (4.163a), which coincides with Eq. (3) if⁶

$$\mathbf{c} = -\gamma \mathcal{B} \frac{\hbar}{2}. \quad (5.13)$$

In particular, if the field \mathcal{B} , and hence the vector \mathbf{c} , is directed along the z -axis and is time-independent, Eqs. (4.170) and (4.173)-(4.174) show that the representation point $\langle \sigma \rangle$ on the Bloch sphere rotates within a plane normal to this axis (see Fig. 3b) with the angular velocity

$$\frac{d\varphi}{dt} \equiv \Omega = -\gamma \mathcal{B}_z \equiv \frac{2c_z}{\hbar}. \quad (5.14)$$

Almost evidently, since the selection of the coordinate axes is arbitrary, this picture should remain valid for any orientation of the vector \mathbf{c} , with the representation point rotating, on the Bloch sphere, around its direction, with the angular speed $|\Omega| = 2c/\hbar$ – see Fig. 3c. This fact may be proved using any picture of the quantum dynamics, discussed in Sec. 4.6. Actually, the reader may already have done that by solving Problems 4.27-4.28, just to see that even for the particular, simple initial state of the system (\uparrow), the final results for the Cartesian components of the vector $\langle \sigma \rangle$ are somewhat bulky. However, this description may be readily simplified, even for an arbitrary time dependence of the “field” vector $\mathbf{c}(t)$ in Eq. (3), by using the geometric vector language.

For that, let us rewrite Eq. (3) (again, with $b = 0$) in the operator form,

$$\hat{H} = \mathbf{c}(t) \cdot \hat{\sigma}, \quad (5.15)$$

valid in an arbitrary basis. According to Eq. (4.199), the corresponding Heisenberg equation of motion for the j^{th} Cartesian components of the vector-operator $\hat{\sigma}$ (which does not depend on time explicitly, $\partial \hat{\sigma} / \partial t = 0$) is

⁶ This correspondence justifies using the use of the term “field” for the vector \mathbf{c} .

$$i\hbar\dot{\hat{\sigma}}_j = [\hat{\sigma}_j, \hat{H}] \equiv [\hat{\sigma}_j, \mathbf{c}(t) \cdot \hat{\boldsymbol{\sigma}}] \equiv \left[\hat{\sigma}_j, \sum_{j'=1}^3 c_{j'}(t) \hat{\sigma}_{j'} \right] \equiv \sum_{j'=1}^3 c_{j'}(t) [\hat{\sigma}_j, \hat{\sigma}_{j'}]. \quad (5.16)$$

Now using the commutation relations (4.155), which remain valid in any basis and in any picture of time evolution,⁷ we get

$$i\hbar\dot{\hat{\sigma}}_j = 2i \sum_{j',j''=1}^3 c_{j'}(t) \hat{\sigma}_{j'} \varepsilon_{jj'j''}, \quad (5.17)$$

where $\varepsilon_{jj'j''}$ is the Levi-Civita symbol. But it is straightforward to verify that the usual vector product of two 3D vectors may be represented in a similar Cartesian-component form:

$$(\mathbf{a} \times \mathbf{b})_j = \begin{vmatrix} \mathbf{n}_1 & \mathbf{n}_2 & \mathbf{n}_3 \\ a_1 & a_2 & a_3 \\ b_1 & b_2 & b_3 \end{vmatrix}_j = \sum_{j',j''=1}^3 a_{j'} b_{j''} \varepsilon_{jj'j''}, \quad (5.18)$$

As a result, the right-hand side of Eq. (17) may be rewritten as $2i[\mathbf{c}(t) \times \hat{\boldsymbol{\sigma}}]_j$, and that relation may be recast in a vector form – or rather several equivalent forms:

$$i\hbar\dot{\hat{\boldsymbol{\sigma}}} = 2i\mathbf{c}(t) \times \hat{\boldsymbol{\sigma}}, \quad \text{or} \quad \dot{\hat{\boldsymbol{\sigma}}} = \frac{2}{\hbar} \mathbf{c}(t) \times \hat{\boldsymbol{\sigma}}, \quad \text{or} \quad \dot{\hat{\boldsymbol{\sigma}}} = \boldsymbol{\Omega}(t) \times \hat{\boldsymbol{\sigma}}, \quad (5.19)$$

where the vector $\boldsymbol{\Omega}$ is defined as

$$\frac{\hbar}{2} \boldsymbol{\Omega}(t) \equiv \mathbf{c}(t) \quad (5.20)$$

– an evident vector generalization of Eq. (14).⁸ As we have seen in Sec. 4.6, any linear relation between two Heisenberg operators is also valid for the expectation values of the corresponding observables, so the last form of Eq. (19) yields:

$$\langle \dot{\hat{\boldsymbol{\sigma}}} \rangle = \boldsymbol{\Omega}(t) \times \langle \hat{\boldsymbol{\sigma}} \rangle. \quad (5.21)$$

But this is the well-known kinematic formula⁹ for the rotation of a constant-length classical 3D vector $\langle \hat{\boldsymbol{\sigma}} \rangle$ around the instantaneous direction of the vector $\boldsymbol{\Omega}(t)$, with the instantaneous angular velocity $\boldsymbol{\Omega}(t)$. So, the time evolution of the representation point on the Bloch sphere is quite simple, especially in the case of a time-independent \mathbf{c} , and hence $\boldsymbol{\Omega}$ – see Fig. 3c.¹⁰ Note that it is sufficient to turn off the field to stop the precession instantly. (Since Eq. (21) is the first-order differential equation, the representation point has no effective inertia.¹¹) Hence, changing the direction and the magnitude of the

⁷ Indeed, if some three operators in the Schrödinger picture are related as $[\hat{A}_S, \hat{B}_S] = \hat{C}_S$, then according to Eq. (4.190), in the Heisenberg picture:

$$[\hat{A}_H, \hat{B}_H] = [\hat{u}^\dagger \hat{A}_H \hat{u}, \hat{u}^\dagger \hat{B}_H \hat{u}] \equiv \hat{u}^\dagger \hat{A}_H \hat{u} \hat{u}^\dagger \hat{B}_H \hat{u} - \hat{u}^\dagger \hat{B}_H \hat{u} \hat{u}^\dagger \hat{A}_H \hat{u} \equiv \hat{u}^\dagger [\hat{A}_S, \hat{B}_S] \hat{u} \equiv \hat{u}^\dagger \hat{C}_S \hat{u} = \hat{C}_H.$$

⁸ It is also easy to verify that in the particular case $\boldsymbol{\Omega} = \Omega \mathbf{n}_z$, Eqs. (19) are reduced, in the z -basis, to Eqs. (4.200) for the spin- $1/2$ vector matrix $\mathbf{S} = (\hbar/2)\boldsymbol{\sigma}$.

⁹ See, e.g., CM Sec. 4.1, in particular Eq. (4.8).

¹⁰ The bulkiness of the solutions of Problems 4.27-4.28 (which were offered just as useful exercises in quantum dynamic formalisms) reflects the awkward expression of the resulting simple circular motion of the vector $\langle \hat{\boldsymbol{\sigma}} \rangle$ (see Fig. 3c) via its Cartesian components.

¹¹ This is also true for the classical angular momentum \mathbf{L} at its torque-induced precession – see, e.g., CM Sec. 4.5.

effective external field, it is possible to drive the representation point of a two-level system from any initial position to any final position on the Bloch sphere, i.e. make the system take any of its possible quantum states.

In the particular case of a spin- $\frac{1}{2}$ in a magnetic field $\mathcal{B}(t)$, it is more customary to use Eqs. (13) and (20) to rewrite Eq. (21) as the following equation for the expectation value of the spin vector $\mathbf{S} = (\hbar/2)\boldsymbol{\sigma}$:

$$\langle \dot{\mathbf{S}} \rangle \equiv \gamma \langle \mathbf{S} \rangle \times \mathcal{B}(t). \quad (5.22)$$

As we know from the discussion in Chapter 4, such a classical description of the spin's evolution does not give a full picture of the quantum reality; in particular, it does not describe the possible large uncertainties of its components – see, e.g., Eqs. (4.135). The situation, however, is different for a collection of $N \gg 1$ similar, non-interacting spins, initially prepared to be in the same state – for example by polarizing all spins with a strong external field \mathcal{B}_0 , at relatively low temperatures T , with $k_B T \ll \gamma \mathcal{B}_0 \hbar$. (A practically important example of such a collection is a set of nuclear spins in macroscopic condensed-matter samples, where the spin interaction with each other and the environment is typically very small.) For such a collection, Eq. (22) is still valid, while the relative uncertainty of the resulting sample's magnetization $\mathbf{M} = n \langle \mathbf{m} \rangle = n \gamma \langle \mathbf{S} \rangle$ (where $n \equiv N/V$ is the spin density) is proportional to $1/N^{1/2} \ll 1$. Thus, the evolution of magnetization may be described, with good precision, by the essentially classical equation:

$$\dot{\mathbf{M}} = \gamma \mathbf{M} \times \mathcal{B}(t). \quad (5.23)$$

This equation, or the equivalent set of three *Bloch equations*¹² for its Cartesian components, with the right-hand side augmented with small terms describing the effects of dephasing and relaxation (to be discussed in Chapter 7), is used, in particular, to describe the *magnetic resonance*, taking place when the frequency (4.164) of the magnetization's precession in a strong dc magnetic field approaches the frequency of an additionally applied (and usually weak) ac/rf field. Two species of this effect, the electron paramagnetic resonance (EPR) and the nuclear magnetic resonance (NMR) are broadly used in material science, chemistry, and medicine. Unfortunately, I will not have time to discuss the related technical issues and methods (in particular, interesting ac/rf pulsing techniques, including the so-called *spin echo* and *Ramsey interferometry*) in detail, and have to refer the reader to special literature.¹³

5.2. The Ehrenfest theorem

In Sec. 4.7, we have derived all the basic relations of wave mechanics from the bra-ket formalism, which will also enable us to get some important additional results in that area. One of them is a pair of very interesting relations, together called the *Ehrenfest theorem*. To derive them, for the simplest case of 1D orbital motion, let us calculate the following commutator:

¹² They were introduced by F. Bloch in the same 1946 paper as the Bloch-sphere representation. In the 1950s when the value of Eq. (21) for quantum optics became recognized, this equation and its open-system generalizations became known as *optical Bloch equations*. Currently, the term 'Bloch equations' is frequently used for any two-level systems, regardless of the physical origin of the Hamiltonian (15).

¹³ For introductions see, e.g., J. Wertz and J. Bolton, *Electron Spin Resonance*, 2nd ed., Wiley, 2007; J. Keeler, *Understanding NMR Spectroscopy*, 2nd ed., Wiley, 2010.

$$[\hat{x}, \hat{p}_x^2] \equiv \hat{x}\hat{p}_x\hat{p}_x - \hat{p}_x\hat{p}_x\hat{x}. \quad (5.24)$$

Let us apply the commutation relation (4.238), in the following form:

$$\hat{x}\hat{p}_x = \hat{p}_x\hat{x} + i\hbar\hat{I}, \quad (5.25)$$

to the first term of the right-hand side of Eq. (24) twice, with the goal to chase the coordinate operator into the rightmost position:

$$\hat{x}\hat{p}_x\hat{p}_x = (\hat{p}_x\hat{x} + i\hbar\hat{I})\hat{p}_x \equiv \hat{p}_x\hat{x}\hat{p}_x + i\hbar\hat{p}_x = \hat{p}_x(\hat{p}_x\hat{x} + i\hbar\hat{I}) + i\hbar\hat{p}_x \equiv \hat{p}_x\hat{p}_x\hat{x} + 2i\hbar\hat{p}_x. \quad (5.26)$$

The first term of this result cancels with the last term of Eq. (24), so the commutator becomes quite simple:

$$[\hat{x}, \hat{p}_x^2] = 2i\hbar\hat{p}_x. \quad (5.27)$$

Let us use this equality to calculate the Heisenberg-picture equation of motion of the operator \hat{x} , by applying the general Heisenberg equation (4.199) to the 1D orbital motion described by the Hamiltonian (4.237), but possibly with a more general, time-dependent potential energy U :

$$\frac{d\hat{x}}{dt} = \frac{1}{i\hbar} [\hat{x}, \hat{H}] = \frac{1}{i\hbar} \left[\hat{x}, \frac{\hat{p}_x^2}{2m} + U(\hat{x}, t) \right]. \quad (5.28)$$

The potential energy operator is a function of the coordinate operator and hence, as we know, commutes with it. Thus, the right-hand side of Eq. (28) is proportional to the commutator (27), and we get

$$\boxed{\frac{d\hat{x}}{dt} = \frac{\hat{p}_x}{m}}. \quad (5.29)$$

Heisenberg
equation
for
coordinate

In this operator equation, we readily recognize the full analog of the classical relation between the particle's momentum and its velocity.

Now let us see what a similar procedure gives for the momentum's derivative:

$$\frac{d\hat{p}_x}{dt} = \frac{1}{i\hbar} [\hat{p}_x, \hat{H}] = \frac{1}{i\hbar} \left[\hat{p}_x, \frac{\hat{p}_x^2}{2m} + U(\hat{x}, t) \right]. \quad (5.30)$$

The kinetic energy operator commutes with the momentum operator and hence drops from the right-hand side of this equation. To calculate the remaining commutator of the momentum and the potential energy, let us use the fact that any smooth (infinitely differentiable) function may be represented by its Taylor expansion:

$$U(\hat{x}, t) = \sum_{k=0}^{\infty} \frac{1}{k!} \frac{\partial^k U}{\partial \hat{x}^k} \hat{x}^k, \quad (5.31)$$

where the derivatives of U may be understood as c -numbers (evaluated at $x = 0$, and the given time t), so we may write

$$[\hat{p}_x, U(\hat{x}, t)] = \sum_{k=0}^{\infty} \frac{1}{k!} \frac{\partial^k U}{\partial \hat{x}^k} [\hat{p}_x, \hat{x}^k] = \sum_{k=0}^{\infty} \frac{1}{k!} \frac{\partial^k U}{\partial \hat{x}^k} \left(\hat{p}_x \underbrace{\hat{x}\hat{x}\dots\hat{x}}_{k \text{ times}} - \underbrace{\hat{x}\hat{x}\dots\hat{x}}_{k \text{ times}} \hat{p}_x \right). \quad (5.32a)$$

Applying Eq. (25) k times to the last term in the parentheses, exactly as we did in Eq. (26), we get

$$[\hat{p}_x, U(\hat{x}, t)] = -\sum_{k=1}^{\infty} \frac{1}{k!} \frac{\partial^k U}{\partial \hat{x}^k} ik\hbar \hat{x}^{k-1} \equiv -i\hbar \sum_{k=1}^{\infty} \frac{1}{(k-1)!} \frac{\partial^k U}{\partial \hat{x}^k} \hat{x}^{k-1}. \quad (5.32b)$$

But the last sum is just the Taylor expansion of the derivative $\partial U/\partial x$. Indeed,

$$\frac{\partial U}{\partial \hat{x}} = \sum_{k'=0}^{\infty} \frac{1}{k'!} \frac{\partial^{k'}}{\partial \hat{x}^{k'}} \left(\frac{\partial U}{\partial \hat{x}} \right) \hat{x}^{k'} = \sum_{k'=0}^{\infty} \frac{1}{k'!} \frac{\partial^{k'+1} U}{\partial \hat{x}^{k'+1}} \hat{x}^{k'} = \sum_{k=1}^{\infty} \frac{1}{(k-1)!} \frac{\partial^k U}{\partial \hat{x}^k} \hat{x}^{k-1}, \quad (5.33)$$

where at the last step, the summation index was changed from k' to $k-1$. As a result, we may recast Eq. (5.32b) as

$$[\hat{p}_x, U(\hat{x}, t)] = -i\hbar \frac{\partial}{\partial \hat{x}} U(\hat{x}, t), \quad (5.34)$$

so Eq. (30) yields:

$$\frac{d\hat{p}_x}{dt} = -\frac{\partial}{\partial \hat{x}} U(\hat{x}, t). \quad (5.35)$$

Heisenberg
equation
for
momentum

This equation also coincides with the classical equation of motion! Moreover, averaging Eqs. (29) and (35) over the initial state (as Eq. (4.191) prescribes), we get similar results for the expectation values:¹⁴

$$\frac{d\langle x \rangle}{dt} = \frac{\langle p_x \rangle}{m}, \quad \frac{d\langle p_x \rangle}{dt} = -\left\langle \frac{\partial U}{\partial x} \right\rangle. \quad (5.36)$$

Ehrenfest
theorem

However, it is important to remember that the similarity of these quantum-mechanical equations and their classical mechanics analogs is superficial, and the degree of difference between the two mechanics very much depends on the problem. As one extreme, let us consider the case when a particle's state, at any moment between t_0 and t , may be accurately represented by one, relatively p_x -narrow wave packet. Then we may interpret Eqs. (36) as the equations of the essentially classical motion of the wave packet's center, and consider this fact as a manifestation of the correspondence principle. However, even in this case, it is important to remember the purely quantum mechanical effects of non-zero wave packet broadening and its spread in time, which were discussed in Sec. 2.2.

As an opposite extreme, let us revisit the “leaky” potential well discussed in Sec. 2.5 – see Fig. 2.15. Since both the potential $U(x)$ and the initial wavefunction of that system are symmetric relative to point $x = 0$ at all times, the right-hand sides of both Eqs. (36) identically equal zero, and hence they predict that the average values of the coordinate and the momentum stay equal to zero at all times. Of course, this prediction is correct, but it does not tell us much about the rich dynamics of the system: the finite lifetime of the metastable state, the formation of two wave packets, their waveform and propagation speed (see Fig. 2.17), and about the insights the full solution gives for the quantum measurement theory and the system's irreversibility. Another similar example is the energy band theory (Sec. 2.7), with its purely quantum effect of the allowed energy bands and forbidden energy gaps, of which Eqs. (36) give no clue.

To summarize, the Ehrenfest theorem is useful as an illustration of the correspondence principle and as the sanity check of quantum-mechanical calculation results, but its predictive power should not be exaggerated.

¹⁴ The equation set (36) constitutes the *Ehrenfest theorem*, named after its author, Paul Ehrenfest.

5.3. The Feynman path integral

As has been already mentioned, even within the realm of wave mechanics, the bra-ket language may simplify some calculations that would be very bulky using the notation used in Chapters 1-3. Probably the best example is the famous alternative, *path-integral* formulation of quantum mechanics.¹⁵ I will review this important concept, cutting one math corner for the sake of brevity.¹⁶ (This shortcut will be clearly marked below.)

Let us inner-multiply both parts of Eq. (4.157a), which is essentially the definition of the time-evolution operator, by the bra-vector of state x ,

$$\langle x | \alpha(t) \rangle = \langle x | \hat{u}(t, t_0) | \alpha(t_0) \rangle, \quad (5.37)$$

insert the identity operator before the ket-vector on the right-hand side, and then use the closure condition in the form of Eq. (4.252), with x' replaced with x_0 :

$$\langle x | \alpha(t) \rangle = \int dx_0 \langle x | \hat{u}(t, t_0) | x_0 \rangle \langle x_0 | \alpha(t_0) \rangle. \quad (5.38)$$

According to Eq. (4.233), this equality may be represented as

$$\Psi_\alpha(x, t) = \int dx_0 \langle x | \hat{u}(t, t_0) | x_0 \rangle \Psi_\alpha(x_0, t_0). \quad (5.39)$$

Comparing this expression with Eq. (2.44), we see that the long bracket in this relation is nothing other than the 1D propagator that was discussed in Sec. 2.2, i.e.

$$G(x, t; x_0, t_0) = \langle x | \hat{u}(t, t_0) | x_0 \rangle. \quad (5.40)$$

Let me hope that the reader sees that this equality corresponds to the physical sense of the propagator.

Now let us break the time segment $[t_0, t]$ into N (for the time being, not necessarily equal) parts by inserting $(N - 1)$ intermediate points (Fig. 4) with

$$t_0 < t_1 < \dots < t_k < \dots < t_{N-1} < t, \quad (5.41)$$

and use the definition (4.157) of the time evolution operator to write

$$\hat{u}(t, t_0) = \hat{u}(t, t_{N-1}) \hat{u}(t_{N-1}, t_{N-2}) \dots \hat{u}(t_2, t_1) \hat{u}(t_1, t_0). \quad (5.42)$$

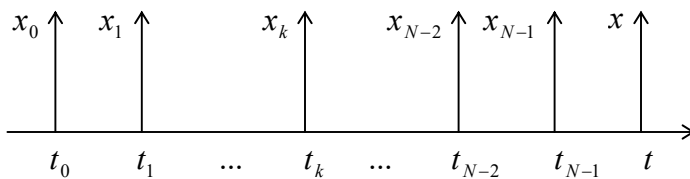


Fig. 5.4. Time partition and coordinate notation at the initial stage of the Feynman path integral's derivation.

¹⁵ This formulation was developed in 1948 by Richard P. Feynman. (According to his memories, this work was motivated by a "mysterious" remark by P. Dirac in his pioneering 1930 textbook on quantum mechanics.)

¹⁶ A more thorough discussion of the path-integral approach may be found in the famous text by R. Feynman and A. Hibbs, *Quantum Mechanics and Path Integrals*, first published in 1965. (For its latest edition by Dover in 2010, the book was emended by D. Styler.) For a more recent monograph, which reviews more applications, see L. Schulman, *Techniques and Applications of Path Integration*, Wiley, 1981.

After plugging Eq. (42) into Eq. (40), let us insert the identity operator, again in the closure form (4.252), but written for x_k rather than x' , between each two partial evolution operators including the time argument t_k . The result is

$$G(x, t; x_0, t_0) = \int dx_{N-1} \int dx_{N-2} \dots \int dx_1 \langle x | \hat{u}(t, t_{N-1}) | x_{N-1} \rangle \langle x_{N-1} | \hat{u}(t_{N-1}, t_{N-2}) | x_{N-2} \rangle \dots \langle x_1 | \hat{u}(t_1, t_0) | x_0 \rangle. \quad (5.43)$$

The physical sense of each integration variable x_k is the wavefunction's argument at time t_k – see Fig. 4.

The key Feynman's step was the realization that if all intervals are taken similar and sufficiently small, $t_k - t_{k-1} = d\tau \rightarrow 0$, all the partial brackets participating in Eq. (43) may be expressed via the free-particle's propagator given by Eq. (2.49), even if the particle is not free, but moves in a stationary potential profile $U(x)$. To show that, let us use either Eq. (4.175) or Eq. (4.181), which, for a small time interval $d\tau$, give the same result:

$$\hat{u}(\tau + d\tau, \tau) = \exp\left\{-\frac{i}{\hbar} \hat{H} d\tau\right\} = \exp\left\{-\frac{i}{\hbar} \left(\frac{\hat{p}^2}{2m} d\tau + U(\hat{x}) d\tau\right)\right\}. \quad (5.44)$$

Generally, an exponent of a sum of two operators may be treated as that of c -number arguments, and in particular factored into a product of two exponents, only if the operators commute. (In that case, we can use all the standard algebra for the exponents of c -number arguments.) In our case, this is not so because the operator $\hat{p}^2/2m$ does not commute with \hat{x} , and hence with $U(\hat{x})$. However, it may be shown¹⁷ that for an infinitesimal time interval $d\tau$, the non-zero commutator

$$\left[\frac{\hat{p}^2}{2m} d\tau, U(\hat{x}) d\tau\right] \neq 0, \quad (5.45)$$

proportional to $(d\tau)^2$, may be ignored in the first, linear approximation in $d\tau$. As a result, we may factor the right-hand side in Eq. (44) by writing

$$\hat{u}(\tau + d\tau, \tau)_{d\tau \rightarrow 0} \rightarrow \exp\left\{-\frac{i}{\hbar} \frac{\hat{p}^2}{2m} d\tau\right\} \exp\left\{-\frac{i}{\hbar} U(\hat{x}) d\tau\right\}. \quad (5.46)$$

(This approximation is very much similar in spirit to the trapezoidal-rule approximation in the usual 1D integration,¹⁸ which is also asymptotically impeccable.)

Since the second exponential function on the right-hand side of Eq. (46) commutes with the coordinate operator, we may move it out of each partial bracket participating in Eq. (43), with $U(x)$ turning into a c -number function:

$$\langle x_{\tau+d\tau} | \hat{u}(\tau + d\tau, \tau) | x_\tau \rangle = \langle x_{\tau+d\tau} | \exp\left\{-\frac{i}{\hbar} \frac{\hat{p}^2}{2m} d\tau\right\} | x_\tau \rangle \exp\left\{-\frac{i}{\hbar} U(x) d\tau\right\}. \quad (5.47)$$

But the remaining bracket is just the propagator of a free particle, so for it, we may use Eq. (2.49):

¹⁷ This is exactly the corner I am going to cut because a strict mathematical proof of this (intuitively evident) statement would take more time/space than I can afford.

¹⁸ See, e.g., MA Eq. (5.2).

$$\langle x_{\tau+d\tau} | \exp\left\{-\frac{i}{\hbar} \frac{\hat{p}^2}{2m} d\tau\right\} | x_\tau \rangle = \left(\frac{m}{2\pi i \hbar d\tau}\right)^{1/2} \exp\left\{i \frac{m(dx)^2}{2\hbar d\tau}\right\}. \tag{5.48}$$

As the result, the full propagator (43) takes the form

$$G(x, t; x_0, t_0) = \lim_{N \rightarrow \infty} \int dx_{N-1} \int dx_{N-2} \dots \int dx_1 \left(\frac{m}{2\pi i \hbar d\tau}\right)^{N/2} \exp\left\{\sum_{k=1}^N \left[i \frac{m(dx)^2}{2\hbar d\tau} - i \frac{U(x)}{\hbar} d\tau \right]_{\tau=t_k}\right\}. \tag{5.49}$$

At $N \rightarrow \infty$ and hence $d\tau \equiv (t - t_0)/N \rightarrow 0$, the sum under the exponent in this expression may be approximated with the corresponding integral:

$$\sum_{k=1}^N \frac{i}{\hbar} \left[\frac{m}{2} \left(\frac{dx}{d\tau}\right)^2 - U(x) \right]_{\tau=t_k} d\tau \rightarrow \frac{i}{\hbar} \int_{t_0}^t \left[\frac{m}{2} \left(\frac{dx}{d\tau}\right)^2 - U(x) \right] d\tau, \tag{5.50}$$

and the expression in the square brackets is just the particle’s Lagrangian function \mathcal{L} .¹⁹ The integral of this function over time is the classical action \mathcal{S} calculated along a particular “path” $x(\tau)$.²⁰ As a result, defining the (1D) *path integral* as

$$\int (\dots) D[x(\tau)] \equiv \lim_{N \rightarrow \infty} \int dx_{N-1} \int dx_{N-2} \dots \int dx_1 (\dots), \tag{5.51a}$$

1D path integral: definition

we can bring our result to the following (superficially simple) form:

$$G(x, t; x_0, t_0) = \int \exp\left\{\frac{i}{\hbar} \mathcal{S}[x(\tau)]\right\} D[x(\tau)]. \tag{5.51b}$$

1D propagator via path integral

The name “path integral” for the mathematical construct (51a) may be readily explained if we keep the number N of time intervals large but still finite, and also approximate each of the enclosed integrals with a sum over $M \gg 1$ discrete points along the coordinate axis – see Fig. 5a.

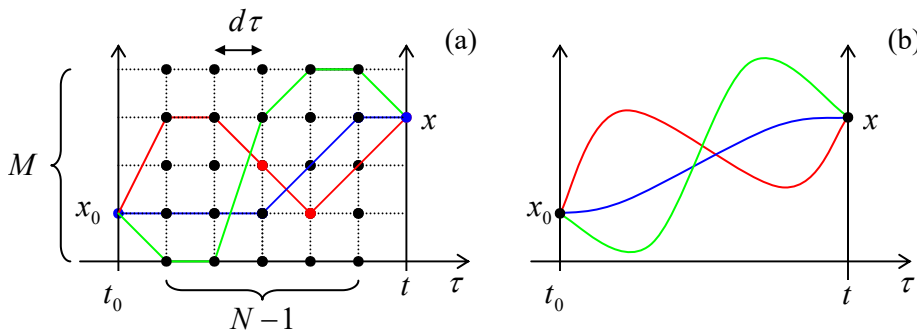


Fig. 5.5. Several 1D classical paths: (a) in the discrete approximation and (b) in the continuous limit.

Then the path integral (51a) is the product of $(N - 1)$ sums corresponding to different values of time τ , each of them with M terms, each of those representing the function under the integral at a particular spatial point. Multiplying those $(N - 1)M$ terms, we get a sum of $(N - 1)M$ terms, each

¹⁹ See, e.g., CM Sec. 2.1.

²⁰ See, e.g., CM Sec. 10.3.

evaluating the function at a specific spatial-temporal point $[x, \tau]$. These terms may be now grouped to represent all possible different continuous classical paths $x[\tau]$ from the initial point $[x_0, t_0]$ to the finite point $[x, t]$. It is evident that the last interpretation remains true even in the continuous limit $N, M \rightarrow \infty$ (see Fig. 5b).

Why does such a path representation of the sum make sense? This is because in the classical limit, the particle follows just a certain path, corresponding to the minimum of the action \mathcal{S}_{cl} . As a result, for all close trajectories, the difference $(\mathcal{S} - \mathcal{S}_{cl})$ is proportional to the square of the deviation from the classical trajectory. Hence, for a quasiclassical motion, with $\mathcal{S}_{cl} \gg \hbar$, there is a bunch of close trajectories, with $(\mathcal{S} - \mathcal{S}_{cl}) \ll \hbar$, that give substantial contributions to the path integral. On the other hand, strongly non-classical trajectories, with $(\mathcal{S} - \mathcal{S}_{cl}) \gg \hbar$, give phases \mathcal{S}/\hbar rapidly oscillating from one trajectory to the next one, and their contributions to the path integral are averaged out.²¹ As a result, for a quasi-classical motion, the propagator's exponent may be evaluated on the classical path only:

$$G_{cl} \propto \exp\left\{\frac{i}{\hbar} \mathcal{S}_{cl}\right\} = \exp\left\{\frac{i}{\hbar} \int_{t_0}^t \left[\frac{m}{2} \left(\frac{dx}{d\tau}\right)^2 - U(x) \right] d\tau\right\}. \quad (5.52)$$

The sum of the kinetic and potential energies is the full energy E of the particle, which remains constant for motion in a stationary potential $U(x)$, so we may rewrite the expression under the last integral as²²

$$\left[\frac{m}{2} \left(\frac{dx}{d\tau}\right)^2 - U(x) \right] d\tau = \left[m \left(\frac{dx}{d\tau}\right)^2 - E \right] d\tau = m \frac{dx}{d\tau} dx - E d\tau. \quad (5.53)$$

With this replacement, Eq. (52) yields

$$G_{cl} \propto \exp\left\{\frac{i}{\hbar} \int_{x_0}^x m \frac{dx}{d\tau} dx\right\} \exp\left\{-\frac{i}{\hbar} E(t-t_0)\right\} = \exp\left\{\frac{i}{\hbar} \int_{x_0}^x p(x) dx\right\} \exp\left\{-\frac{i}{\hbar} E(t-t_0)\right\}, \quad (5.54)$$

where p is the classical momentum of the particle. But (at least, leaving the pre-exponential factor alone) this is the WKB approximation result that was derived and studied in detail in Chapter 2!

One may question the value of such a complicated calculation, which yields results that could be readily obtained from Schrödinger's wave mechanics. Feynman's approach is indeed not used too often, but it has its merits. First, it has an important philosophical (and hence heuristic) value. Indeed, Eq. (51) may be interpreted by saying that the essence of quantum mechanics is the exploration, by the system, of all possible paths $x(\tau)$, each of them classical-like, in the sense that the particle's coordinate x and velocity $dx/d\tau$ are exactly defined simultaneously at each point. The resulting contributions to the path integral are added up coherently to form the actual propagator G , and via it, the final probability $W \propto |G|^2$ of the particle's propagation from $[x_0, t_0]$ to $[x, t]$. As the scale of the action \mathcal{S} of the motion

²¹ This fact may be proved by expanding the difference $(\mathcal{S} - \mathcal{S}_{cl})$ in the Taylor series in the path variation (leaving only the leading quadratic terms) and working out the resulting Gaussian integrals. This integration, together with the pre-exponential coefficient in Eq. (51a), gives exactly the pre-exponential factor that we have already found refining the WKB approximation in Sec. 2.4.

²² The same trick is often used in analytical classical mechanics – say, for proving the Hamilton principle, and for the derivation of the Hamilton-Jacobi equations – see, e.g., CM Secs. 10.3-4.

decreases and becomes comparable to \hbar , more and more paths produce substantial contributions to this sum, and hence to W , providing a larger and larger difference between the quantum and classical properties of the system.

Second, the path integral provides a justification for some simple explanations of quantum phenomena. A typical example is the quantum interference effects discussed in Sec. 3.1 – see, e.g., Fig. 3.1 and the corresponding text. In that discussion, we used the Huygens principle to argue that at the two-slit interference, the WKB approximation might be restricted to contributions from two paths that pass through different slits, but otherwise consist of straight-line segments. To have another look at that assumption, let us generalize the path integral to multi-dimensional geometries. Fortunately, the simple structure of Eq. (51b) makes such generalization virtually evident:

$$G(\mathbf{r}, t; \mathbf{r}_0, t_0) = \int \exp\left\{\frac{i}{\hbar} \mathcal{S}[\mathbf{r}(\tau)]\right\} D[\mathbf{r}(\tau)], \quad \mathcal{S} \equiv \int_{t_0}^t \mathcal{L}\left(\mathbf{r}, \frac{d\mathbf{r}}{d\tau}\right) d\tau = \int_{t_0}^t \left[\frac{m}{2} \left(\frac{d\mathbf{r}}{d\tau}\right)^2 - U(\mathbf{r}) \right] d\tau. \quad (5.55)$$

3D propagator as a path integral

where the definition (51a) of the path integral should be also modified correspondingly. (I will not go into these technical details.) For the Young-type experiment (Fig. 3.1), where a classical particle could reach the detector only after passing through one of the slits, the classical paths dominating the contribution from each slit are the straight-line segments shown in Fig. 3.1, and if they are much longer than the de Broglie wavelength, the propagator may be well approximated by the sum of two integrals of $\mathcal{L}d\tau = i\mathbf{p}(\mathbf{r}) \cdot d\mathbf{r} / \hbar$ – just as this was done in Sec. 3.1.

Last but not least, the path integral allows simple solutions to some problems that would be hard to obtain by other methods. As the simplest example, let us consider the problem of tunneling in multi-dimensional space, sketched in Fig. 6 for the 2D case – just for the graphics’ simplicity. Here, the potential profile $U(x, y)$ has a saddle-like shape. (Another helpful image is a mountain path between two summits, in Fig. 6 located on the top and at the bottom of the shown region.) A particle of energy E may move classically in the left and right regions with $U(x, y) < E$, but if E is not sufficiently high, it can pass from one of these regions to another one only via the quantum-mechanical tunneling under the pass. Let us calculate the transparency of this potential barrier in the WKB approximation, ignoring the possible pre-exponential factor.²³

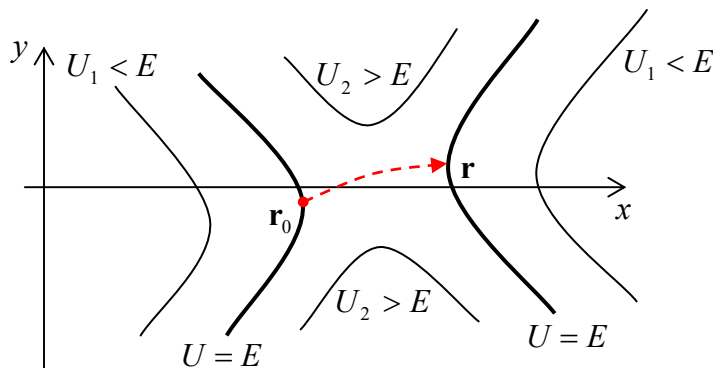


Fig. 5.6. A saddle-type 2D potential profile and the instanton trajectory of a particle of energy E (schematically).

²³ Actually, one can argue that the pre-exponential factor should be close to 1, just like in Eq. (2.117), especially if the potential is smooth, in the sense of Eq. (2.107), in all spatial directions. (Let me remind the reader that for most practical applications of quantum tunneling, the pre-exponential factor is of relatively minor importance.)

According to the evident multi-dimensional generalization Eq. (54), for the classically forbidden region, where $E < U(x, y)$, and hence $\mathbf{p}(\mathbf{r})/\hbar = i\boldsymbol{\kappa}(\mathbf{r})$, the contributions to the propagator (55) are proportional to

$$e^{-I} \exp\left\{-\frac{i}{\hbar} E(t-t_0)\right\}, \quad \text{where } I \equiv \int_{\mathbf{r}_0}^{\mathbf{r}} \boldsymbol{\kappa}(\mathbf{r}) \cdot d\mathbf{r}, \quad (5.56)$$

where $\kappa \equiv |\boldsymbol{\kappa}|$ may be calculated just in the 1D case – cf. Eq. (2.97):

$$\frac{\hbar^2 \kappa^2(\mathbf{r})}{2m} = U(\mathbf{r}) - E. \quad (5.57)$$

Hence the path integral in this region is much simpler than in the classically allowed region because the spatial exponents are purely real and there is no complex interference between them. Due to the minus sign before I in the exponent (56), the *largest* contribution to G evidently comes from the trajectory (or a narrow bundle of close trajectories) for which the integral I has the *smallest* value, so the barrier transparency may be calculated as

3D
tunneling
in WKB
limit

$$\mathcal{T} \approx |G|^2 \approx e^{-2I} \equiv \exp\left\{-2 \int_{\mathbf{r}_0}^{\mathbf{r}} \boldsymbol{\kappa}(\mathbf{r}') \cdot d\mathbf{r}'\right\}, \quad (5.58)$$

where \mathbf{r} and \mathbf{r}_0 are certain points on the opposite classical turning-point surfaces: $U(\mathbf{r}) = U(\mathbf{r}_0) = E$ – see Fig. 6.

Thus the barrier transparency problem is reduced to finding the trajectory (including the points \mathbf{r} and \mathbf{r}_0) that connects these two surfaces and minimizes the functional I . This is of course a well-known problem of the calculus of variations,²⁴ but it is interesting that the path integral provides a simple alternative way of solving it. Let us consider an auxiliary problem of particle's motion in the potential profile $U_{\text{inv}}(\mathbf{r})$ that is *inverted* relative to the particle's energy E , i.e. is defined by the following equality:

$$U_{\text{inv}}(\mathbf{r}) - E \equiv E - U(\mathbf{r}). \quad (5.59)$$

As was discussed above, at fixed energy E , the path integral for the WKB motion in the classically allowed region of potential $U_{\text{inv}}(x, y)$ (that coincides with the classically forbidden region of the original problem) is dominated by the classical trajectory corresponding to the minimum of

$$\mathcal{S}_{\text{inv}} = \int_{\mathbf{r}_0}^{\mathbf{r}} \mathbf{p}_{\text{inv}}(\mathbf{r}') \cdot d\mathbf{r}' = \hbar \int_{\mathbf{r}_0}^{\mathbf{r}} \mathbf{k}_{\text{inv}}(\mathbf{r}') \cdot d\mathbf{r}', \quad (5.60)$$

where \mathbf{k}_{inv} should be determined from the WKB relation

$$\frac{\hbar^2 k_{\text{inv}}^2(\mathbf{r})}{2m} \equiv E - U_{\text{inv}}(\mathbf{r}). \quad (5.61)$$

But comparing Eqs. (57), (59), and (61), we see that $\mathbf{k}_{\text{inv}} = \boldsymbol{\kappa}$ at each point! This means that in the WKB limit, the tunneling path corresponds to the classical (so-called *instanton*²⁵) trajectory of the same

²⁴ For a concise introduction to the field see, e.g., I. Gelfand and S. Fomin, *Calculus of Variations*, Dover, 2000, or L. Elsgolc, *Calculus of Variations*, Dover, 2007.

²⁵ In the quantum field theory, the instanton concept may be formulated somewhat differently and has more complex applications – see, e.g. R. Rajaraman, *Solitons and Instantons*, North-Holland, 1987.

particle moving in the inverted potential $U_{\text{inv}}(\mathbf{r})$. If the initial point \mathbf{r}_0 is fixed, this trajectory may be readily found by means of classical mechanics. (Note that the initial kinetic energy, and hence the initial velocity of the instanton launched from point \mathbf{r}_0 should be zero because by the classical turning point definition, $U_{\text{inv}}(\mathbf{r}_0) = U(\mathbf{r}_0) = E$.) Thus the problem is further reduced to a simpler task of maximizing the transparency (58) by choosing the optimal position of \mathbf{r}_0 on the equipotential surface $U(\mathbf{r}_0) = E$ – see Fig. 6. Moreover, for many symmetric potentials, the position of this point may be readily guessed even without calculations – as it is in Problems 6 and 7, left for the reader’s exercise.

Note that besides the calculation of the potential barrier’s transparency, the instanton trajectory has one more important implication: the so-called *traversal time* τ_t of the classical motion along it, from the point \mathbf{r}_0 to the point \mathbf{r} , in the inverted potential defined by Eq. (59), plays the role of the most important (though not the only one) time scale of the particle’s tunneling under the barrier.²⁶

5.4. Revisiting harmonic oscillator

Now let us return to the 1D harmonic oscillator, which may be understood as any system, regardless of its physical nature, described by the Hamiltonian (4.237) with the potential energy (2.111):

$$\hat{H} = \frac{\hat{p}^2}{2m} + \frac{m\omega_0^2 \hat{x}^2}{2}. \quad (5.62)$$

Harmonic oscillator: Hamiltonian

In Sec. 2.9 we have used a “brute-force” (wave-mechanics) approach to analyze the eigenfunctions $\psi_n(x)$ and eigenvalues E_n of this Hamiltonian, and found that, unfortunately, this approach required relatively complex mathematics, which does not enable an easy calculation of the key characteristics of the system. Fortunately, the bra-ket formalism helps to make such calculations.

First, by introducing the normalized (dimensionless) operators of coordinates and momentum:²⁷

$$\hat{\xi} \equiv \frac{\hat{x}}{x_0}, \quad \hat{\zeta} \equiv \frac{\hat{p}}{m\omega_0 x_0}, \quad (5.63)$$

where $x_0 \equiv (\hbar/m\omega_0)^{1/2}$ is the natural coordinate scale discussed in detail in Sec. 2.9, we can represent the Hamiltonian (62) in a very simple and $x \leftrightarrow p$ symmetric form:

$$\hat{H} = \frac{\hbar\omega_0}{2} (\hat{\xi}^2 + \hat{\zeta}^2). \quad (5.64)$$

This symmetry, as well as our discussion of the very similar coordinate and momentum representations in Sec. 4.7, hints that much may be gained by treating the operators $\hat{\xi}$ and $\hat{\zeta}$ on equal footing. Inspired by this clue, let us introduce a new operator

$$\hat{a} \equiv \frac{\hat{\xi} + i\hat{\zeta}}{\sqrt{2}} \equiv \left(\frac{m\omega_0}{2\hbar} \right)^{1/2} \left(\hat{x} + i \frac{\hat{p}}{m\omega_0} \right). \quad (5.65a)$$

Annihilation operator: definition

²⁶ For more on this interesting issue see, e.g., M. Buttiker and R. Landauer, *Phys. Rev. Lett.* **49**, 1739 (1982), and references therein.

²⁷ This normalization is not really necessary, it just makes the following calculations less bulky – and thus more aesthetically appealing.

Since both operators $\hat{\xi}$ and $\hat{\zeta}$ correspond to real observables, i.e. have real eigenvalues and hence are Hermitian (self-adjoint), the Hermitian conjugate of the operator \hat{a} is simply its complex conjugate:

Creation operator: definition

$$\hat{a}^\dagger \equiv \frac{\hat{\xi} - i\hat{\zeta}}{\sqrt{2}} \equiv \left(\frac{m\omega_0}{2\hbar}\right)^{1/2} \left(\hat{x} - i\frac{\hat{p}}{m\omega_0}\right). \quad (5.65b)$$

Because of the reason that will be clear very soon, \hat{a}^\dagger and \hat{a} (in this order!) are called the *creation and annihilation operators*.

Now solving the simple system of two linear equations (65) for $\hat{\xi}$ and $\hat{\zeta}$, we get the following reciprocal relations:

$$\hat{\xi} = \frac{\hat{a} + \hat{a}^\dagger}{\sqrt{2}}, \quad \hat{\zeta} = \frac{\hat{a} - \hat{a}^\dagger}{\sqrt{2}i}, \quad \text{i.e. } \hat{x} = \left(\frac{\hbar}{m\omega_0}\right)^{1/2} \frac{\hat{a} + \hat{a}^\dagger}{\sqrt{2}}, \quad \hat{p} = (\hbar m\omega_0)^{1/2} \frac{\hat{a} - \hat{a}^\dagger}{\sqrt{2}i}. \quad (5.66)$$

Our Hamiltonian (64) includes only squares of these operators. Calculating them, we have to be careful to avoid swapping the new operators, because they do not commute. Indeed, for the normalized operators (63), Eq. (2.14) gives

$$[\hat{\xi}, \hat{\zeta}] \equiv \frac{1}{x_0^2 m \omega_0} [\hat{x}, \hat{p}] = i\hat{I}, \quad (5.67)$$

so Eqs. (65) yield

Creation-annihilation operators: commutation relation

$$[\hat{a}, \hat{a}^\dagger] = \frac{1}{2} [(\hat{\xi} + i\hat{\zeta}), (\hat{\xi} - i\hat{\zeta})] = -\frac{i}{2} ([\hat{\xi}, \hat{\zeta}] - [\hat{\zeta}, \hat{\xi}]) = \hat{I}. \quad (5.68)$$

With such due caution, Eq. (66) gives

$$\hat{\xi}^2 = \frac{1}{2} \left(\hat{a}^2 + \hat{a}^{\dagger 2} + \hat{a}\hat{a}^\dagger + \hat{a}^\dagger\hat{a} \right), \quad \hat{\zeta}^2 = -\frac{1}{2} \left(\hat{a}^2 + \hat{a}^{\dagger 2} - \hat{a}\hat{a}^\dagger - \hat{a}^\dagger\hat{a} \right). \quad (5.69)$$

Plugging these expressions back into Eq. (64), we get

$$\hat{H} = \frac{\hbar\omega_0}{2} \left(\hat{a}\hat{a}^\dagger + \hat{a}^\dagger\hat{a} \right). \quad (5.70)$$

This expression is elegant enough but may be recast into an even more convenient form. For that, let us rewrite the commutation relation (68) as

$$\hat{a}\hat{a}^\dagger = \hat{a}^\dagger\hat{a} + \hat{I}, \quad (5.71)$$

and plug it into Eq. (70). The result is

$$\hat{H} = \frac{\hbar\omega_0}{2} \left(2\hat{a}^\dagger\hat{a} + \hat{I} \right) \equiv \hbar\omega_0 \left(\hat{N} + \frac{1}{2}\hat{I} \right), \quad (5.72)$$

where, in the last form, one more (evidently, Hermitian) operator

Number operator: definition

$$\hat{N} \equiv \hat{a}^\dagger\hat{a} \quad (5.73)$$

has been introduced. Since, according to Eq. (72), the operators \hat{H} and \hat{N} differ only by the addition of the identity operator and multiplication by a *c*-number, these operators commute. Hence, according to

the general arguments of Sec. 4.5, they share a set of stationary eigenstates n (they are frequently called the *Fock states*), and we can write the standard eigenproblem (4.68) for the new operator as

$$\hat{N}|n\rangle = N_n|n\rangle, \tag{5.74}$$

where N_n are some eigenvalues that, according to Eq. (72), determine also the energy spectrum of the oscillator:

$$E_n = \hbar\omega_0\left(N_n + \frac{1}{2}\right). \tag{5.75}$$

So far, we know only that all eigenvalues N_n are real; to calculate them, let us carry out the following calculation – splendid in its simplicity and efficiency. Consider the result of the action of the operator \hat{N} on the ket-vector $\hat{a}^\dagger|n\rangle$. Using the definition (73) and then the associative rule of the bra-ket formalism, we may write

$$\hat{N}\left(\hat{a}^\dagger|n\rangle\right) \equiv \left(\hat{a}^\dagger\hat{a}\right)\left(\hat{a}^\dagger|n\rangle\right) = \hat{a}^\dagger\left(\hat{a}\hat{a}^\dagger\right)|n\rangle. \tag{5.76}$$

Now using the commutation relation (71), and then Eq. (74), we may continue as

$$\hat{a}^\dagger\left(\hat{a}\hat{a}^\dagger\right)|n\rangle = \hat{a}^\dagger\left(\hat{a}^\dagger\hat{a} + \hat{I}\right)|n\rangle = \hat{a}^\dagger\left(\hat{N} + \hat{I}\right)|n\rangle = \hat{a}^\dagger\left(N_n + 1\right)|n\rangle = \left(N_n + 1\right)\left(\hat{a}^\dagger|n\rangle\right). \tag{5.77}$$

For clarity, let us summarize the result of this calculation:

$$\hat{N}\left(\hat{a}^\dagger|n\rangle\right) = \left(N_n + 1\right)\left(\hat{a}^\dagger|n\rangle\right). \tag{5.78}$$

Performing a similar calculation for the operator \hat{a} , we get a similar formula, but with a different sign:

$$\hat{N}\left(\hat{a}|n\rangle\right) = \left(N_n - 1\right)\left(\hat{a}|n\rangle\right). \tag{5.79}$$

It is time to stop the calculations for a minute, and translate their results into plain English: if $|n\rangle$ is the eigenket of the operator \hat{N} with an eigenvalue N_n , then $\hat{a}^\dagger|n\rangle$ and $\hat{a}|n\rangle$ are also eigenkets of that operator, with the eigenvalues $(N_n + 1)$ and $(N_n - 1)$, respectively. This statement may be vividly represented by the so-called *ladder diagram* shown in Fig. 7.

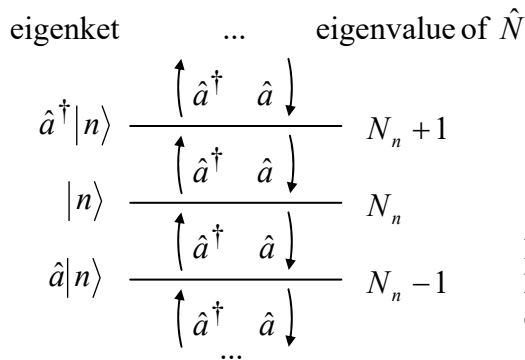


Fig. 5.7. The “ladder diagram” of eigenstates of a 1D harmonic oscillator. Arrows show the actions of the creation and annihilation operators on the eigenstates.

The operator \hat{a}^\dagger moves the system one step up this ladder, while the operator \hat{a} brings it one step down. In other words, the former operator creates a new *excitation* of the system,²⁸ while the latter operator kills (“annihilates”) such excitation.²⁹ On the other hand, according to Eq. (74) inner-multiplied by the bra-vector $\langle n|$, the operator \hat{N} does not change the state of the system, but “counts” its position on the ladder:

$$\langle n|\hat{N}|n\rangle = \langle n|N_n|n\rangle = N_n. \quad (5.80)$$

This is why \hat{N} is called the *number operator*, in our current context meaning the number of the elementary excitations of the oscillator.

This calculation still needs completion. Indeed, we still do not know whether the ladder shown in Fig. 7 shows *all* eigenstates of the oscillator, and what exactly the numbers N_n are. Fascinating enough, both questions may be answered by exploring just one paradox. Let us start with some state n (read: a step of the ladder), and keep going down the ladder, applying the operator \hat{a} again and again. According to Eq. (79), at each step, the eigenvalue N_n is decreased by one, so eventually, it should become negative. However, this cannot happen because any actual eigenstate, including the states represented by kets $|d\rangle \equiv \hat{a}|n\rangle$ and $|n\rangle$, should have a positive norm – see Eq. (4.16). Comparing the norms,

$$\|n\|^2 = \langle n|n\rangle, \quad \|d\|^2 = \langle n|\hat{a}^\dagger \hat{a}|n\rangle = \langle n|\hat{N}|n\rangle = N_n \langle n|n\rangle, \quad (5.81)$$

we see that both of them cannot be positive simultaneously if N_n is negative.

To resolve this paradox let us notice that the action of the creation and annihilation operators on the stationary states n may consist of not only their promotion to an adjacent step of the ladder diagram but also by their multiplication by some c -numbers:

$$\hat{a}|n\rangle = A_n|n-1\rangle, \quad \hat{a}^\dagger|n\rangle = A'_n|n+1\rangle. \quad (5.82)$$

(The linear relations (78)-(79) clearly allow that.) Let us calculate the coefficients A_n assuming, for convenience, that all eigenstates, including the states n and $(n-1)$, are normalized:

$$\langle n|n\rangle = 1, \quad \langle n-1|n-1\rangle = \langle n|\frac{\hat{a}^\dagger}{A_n^*} \frac{\hat{a}}{A_n}|n\rangle = \frac{1}{A_n^* A_n} \langle n|\hat{N}|n\rangle = \frac{N_n}{A_n^* A_n} \langle n|n\rangle = 1. \quad (5.83)$$

From here, we get $|A_n| = (N_n)^{1/2}$, i.e.

$$\hat{a}|n\rangle = N_n^{1/2} e^{i\varphi_n} |n-1\rangle, \quad (5.84)$$

where φ_n is an arbitrary real phase. Now let us consider what happens if all numbers N_n are integers. (Because of the definition of N_n , given by Eq. (74), it is convenient to call these integers n , i.e. to use the same letter as for the corresponding eigenstate.) Then when we have come down to the state with $n = 0$, an attempt to make one more step down gives

$$\hat{a}|0\rangle = 0|-1\rangle. \quad (5.85)$$

²⁸ For electromagnetic field oscillators, such excitations are called *photons*; for mechanical wave oscillators, *phonons*, etc.

²⁹ This is exactly why \hat{a}^\dagger is called the *creation operator*, and \hat{a} , the *annihilation operator*.

But according to Eq. (4.9), the state on the right-hand side of this equation is the “null state”, i.e. does not exist.³⁰ This gives the (only known :-) resolution of the state ladder paradox: the ladder has the lowest step with $N_n = n = 0$.

As a by-product of our discussion, we have obtained a very important relation $N_n = n$, which means, in particular, that the state ladder shown in Fig. 7 includes *all* eigenstates of the oscillator. Plugging this relation into Eq. (75), we see that the *full* spectrum of eigenenergies of the harmonic oscillator is described by the simple formula

$$E_n = \hbar\omega_0 \left(n + \frac{1}{2} \right), \quad n = 0, 1, 2, \dots, \quad (5.86)$$

which was already discussed in Sec. 2.9. It is rather remarkable that the bra-ket formalism has allowed us to derive it without calculating the corresponding (rather cumbersome) wavefunctions $\psi_n(x)$ – see Eqs. (2.284).

Moreover, this formalism may be also used to calculate virtually any matrix element of the oscillator, without using $\psi_n(x)$. However, to do that, we should first calculate the coefficient A'_n participating in the second of Eqs. (82). This may be done similarly to the above calculation of A_n ; alternatively, since we already know that $|A_n| = (N_n)^{1/2} = n^{1/2}$, we may notice that according to Eqs. (73) and (82), the eigenproblem (74), which in our new notation for N_n becomes

$$\hat{N}|n\rangle = n|n\rangle, \quad (5.87)$$

may be rewritten as

$$\hat{N}|n\rangle \equiv \hat{a}^\dagger \hat{a}|n\rangle = \hat{a}^\dagger A_n |n-1\rangle = A_n A'_{n-1} |n\rangle. \quad (5.88)$$

Comparing the right-hand sides of Eqs. (87) and (88), we see that $|A'_{n-1}| = n/|A_n| = n^{1/2}$, i.e. $A'_n = (n+1)^{1/2} \exp(i\varphi_n)$. Taking all phases φ_n and φ_n' equal to zero for simplicity, we may spell out Eqs. (82) as³¹

$$\hat{a}^\dagger |n\rangle = (n+1)^{1/2} |n+1\rangle, \quad \hat{a}|n\rangle = n^{1/2} |n-1\rangle. \quad (5.89)$$

Fock state ladder

Now we can use these formulas to calculate, for example, the matrix elements of the operator \hat{x} in the Fock state basis:

$$\begin{aligned} \langle n' | \hat{x} | n \rangle &\equiv x_0 \langle n' | \hat{\xi} | n \rangle = \frac{x_0}{\sqrt{2}} \langle n' | (\hat{a} + \hat{a}^\dagger) | n \rangle = \frac{x_0}{\sqrt{2}} \left(\langle n' | \hat{a} | n \rangle + \langle n' | \hat{a}^\dagger | n \rangle \right) \\ &= \frac{x_0}{\sqrt{2}} \left[n^{1/2} \langle n' | n-1 \rangle + (n+1)^{1/2} \langle n' | n+1 \rangle \right]. \end{aligned} \quad (5.90)$$

Taking into account the Fock state orthonormality:

$$\langle n' | n \rangle = \delta_{n'n}, \quad (5.91)$$

this result becomes

³⁰ Please note again the radical difference between the null state on the right-hand side of Eq. (85) and the state described by the ket-vector $|0\rangle$ on the left-hand side of that relation. The latter state *does* exist and, moreover, represents the most important, ground state of the system, with $n = 0$ – see Eqs. (2.274)-(2.275).

³¹ A useful mnemonic rule for these key relations is that the *c*-number coefficient in any of them is equal to the square root of the *largest* number of the two states it relates.

Coordinate's
matrix
elements

$$\langle n' | \hat{x} | n \rangle = \frac{x_0}{\sqrt{2}} \left[n^{1/2} \delta_{n',n-1} + (n+1)^{1/2} \delta_{n',n+1} \right] \equiv \left(\frac{\hbar}{2m\omega_0} \right)^{1/2} \left[n^{1/2} \delta_{n',n-1} + (n+1)^{1/2} \delta_{n',n+1} \right]. \quad (5.92)$$

Acting absolutely similarly, for the momentum's matrix elements we get a similar expression:

$$\langle n' | \hat{p} | n \rangle = i \left(\frac{\hbar m \omega_0}{2} \right)^{1/2} \left[-n^{1/2} \delta_{n',n-1} + (n+1)^{1/2} \delta_{n',n+1} \right] \quad (5.93)$$

Hence the matrices of both operators in the Fock-state basis have only two diagonals adjacent to the main diagonal; all other elements (including the main-diagonal ones) are zeros.

The matrix elements of higher powers of these operators, as well as their products, may be handled similarly, though the higher the power, the bulkier the result. For example,

$$\begin{aligned} \langle n' | \hat{x}^2 | n \rangle &= \langle n' | \hat{x} \hat{x} | n \rangle = \sum_{n''=0}^{\infty} \langle n' | \hat{x} | n'' \rangle \langle n'' | \hat{x} | n \rangle \\ &= \frac{x_0^2}{2} \sum_{n''=0}^{\infty} \left[(n'')^{1/2} \delta_{n',n''-1} + (n''+1)^{1/2} \delta_{n',n''+1} \right] \left[n^{1/2} \delta_{n'',n-1} + (n+1)^{1/2} \delta_{n'',n+1} \right] \\ &= \frac{x_0^2}{2} \left\{ [n(n-1)]^{1/2} \delta_{n',n-2} + [(n+1)(n+2)]^{1/2} \delta_{n',n+2} + (2n+1) \delta_{n',n} \right\}. \end{aligned} \quad (5.94)$$

For applications, the most important of these matrix elements are those on its main diagonal:

$$\langle x^2 \rangle \equiv \langle n | \hat{x}^2 | n \rangle = \frac{x_0^2}{2} (2n+1). \quad (5.95)$$

This expression shows, in particular, that the expectation value of the oscillator's potential energy in the n^{th} Fock state is

$$\langle U \rangle \equiv \frac{m\omega_0^2}{2} \langle x^2 \rangle = \frac{m\omega_0^2 x_0^2}{2} \left(n + \frac{1}{2} \right) \equiv \frac{\hbar\omega_0}{2} \left(n + \frac{1}{2} \right). \quad (5.96)$$

This is exactly one-half of the total energy (86) of the oscillator. As a sanity check, an absolutely similar calculation for the momentum squared, and hence for the kinetic energy $p^2/2m$, yields

$$\langle p^2 \rangle = \langle n | \hat{p}^2 | n \rangle = (m\omega_0 x_0)^2 \left(n + \frac{1}{2} \right) \equiv \hbar m \omega_0 \left(n + \frac{1}{2} \right), \quad \text{so} \quad \left\langle \frac{p^2}{2m} \right\rangle = \frac{\hbar\omega_0}{2} \left(n + \frac{1}{2} \right), \quad (5.97)$$

i.e. both partial energies are equal to $E_n/2$, just as in a classical oscillator.³²

Note that according to Eqs. (92) and (93), the expectation values of both x and p in any Fock state are equal to zero:

$$\langle x \rangle \equiv \langle n | \hat{x} | n \rangle = 0, \quad \langle p \rangle \equiv \langle n | \hat{p} | n \rangle = 0, \quad (5.98)$$

³² Still note that operators of the partial (potential and kinetic) energies do *not* commute with either each other or with the full-energy (Hamiltonian) operator, so the Fock states n are *not* their eigenstates. This fact maps onto the well-known oscillations of these partial energies (with the frequency $2\omega_0$) in a classical oscillator, at the full energy staying constant.

This is why, according to the general Eqs. (1.33)-(1.34), the results (95) and (97) also give the variances of the coordinate and the momentum, i.e. the squares of their uncertainties, $(\delta x)^2$ and $(\delta p)^2$. In particular, for the ground state ($n = 0$), these uncertainties are

$$\delta x = \frac{x_0}{\sqrt{2}} \equiv \left(\frac{\hbar}{2m\omega_0} \right)^{1/2}, \quad \delta p = \frac{m\omega_0 x_0}{\sqrt{2}} \equiv \left(\frac{\hbar m\omega_0}{2} \right)^{1/2}. \quad (5.99)$$

In the theory of precise measurements (to be reviewed in brief in Chapter 10), these expressions are often called the *standard quantum limit*.

5.5. Glauber states and squeezed states

There is a huge difference between a quantum stationary (Fock) state of the oscillator and its classical state. Indeed, let us write the well-known classical equations of motion of the oscillator (using capital letters to distinguish classical variables from the arguments of quantum wavefunctions):³³

$$\dot{X} = \frac{P}{m}, \quad \dot{P} = -\frac{\partial U}{\partial x} = -m\omega_0^2 X. \quad (5.100)$$

The simplest method to solve these equations is to introduce the dimensionless complex variable

$$\alpha(t) \equiv \frac{1}{\sqrt{2}x_0} \left[X(t) + i \frac{P(t)}{m\omega_0} \right], \quad (5.101)$$

With this definition, Eqs. (100) are conveniently merged into one equation,

$$\dot{\alpha} = -i\omega_0 \alpha, \quad (5.102)$$

with an evident, very simple solution

$$\alpha(t) = \alpha(0) \exp\{-i\omega_0 t\}, \quad (5.103)$$

so per Eq. (102):

$$X(t) = \sqrt{2}x_0 \operatorname{Re}[\alpha(0) \exp\{-i\omega_0 t\}], \quad P(t) = \sqrt{2}m\omega_0 x_0 \operatorname{Im}[\alpha(0) \exp\{-i\omega_0 t\}],$$

where the constant $\alpha(0)$ is just the (normalized) classical complex amplitude of the oscillations, so their real amplitude is $A = \sqrt{2}x_0 |\alpha(t)| = \sqrt{2}x_0 |\alpha(0)|$.³⁴ By the appropriate choice of the time origin, the complex amplitude may be always made real; then $X \propto \cos\omega_0 t$ and $P \propto -\sin\omega_0 t$.

On the so-called *phase plane*, with the Cartesian coordinates x and p , this solution describes a clockwise rotation of the representation point $\{X(t), P(t)\}$ along an elliptic trajectory starting from the initial point $\{X(0), P(0)\}$. The normalization of the momentum by $m\omega_0$, similar to the one performed by the second of Eqs. (63), makes this trajectory pleasingly circular, with a constant radius equal to the oscillation amplitude A , corresponding to the constant full energy

$$E = \frac{m\omega_0^2}{2} A^2, \quad \text{with } A^2 = [X(t)]^2 + \left[\frac{P(t)}{m\omega_0} \right]^2 = \text{const} = [X(0)]^2 + \left[\frac{P(0)}{m\omega_0} \right]^2, \quad (5.104)$$

³³ If Eqs. (100) are not evident, please consult a classical mechanics course – e.g., CM Sec. 3.2 and/or Sec. 10.1.

³⁴ See, e.g., CM Chapter 5, especially Eqs. (5.4).

determined by the initial conditions – see Fig. 8.)

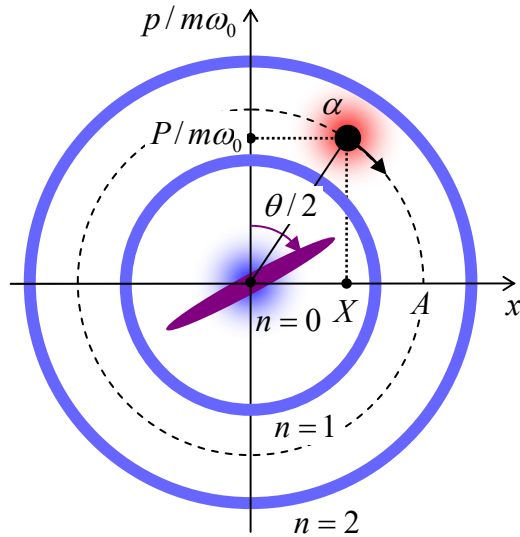


Fig. 5.8. Representations of various states of a harmonic oscillator on the phase plane. The bold black point represents a classical state with displacement amplitude A , with the dashed line showing its trajectory. The (very imperfect) classical images of the Fock states with $n = 0, 1$, and 2 are shown in blue. The blurred red spot is the (equally schematic) image of the Glauber state α , with $|\alpha| = A/\sqrt{2}x_0$. Finally, the magenta elliptical spot is a classical image of a *squeezed* ground state – see below. Arrows show the direction of the states' evolution in time.

On the other hand, according to the basic Eq. (4.161), the time dependence of a Fock state, as of a stationary state of the oscillator, is limited to the phase factor $\exp\{-iE_n t/\hbar\}$. This factor drops out at the averaging (4.125) for any observable. As a result, in this state the expectation values of x , p , or any function thereof are time-independent; moreover, as Eqs. (98) show, $\langle x \rangle = \langle p \rangle = 0$. Taking into account Eqs. (96)-(97), the closest (though very imperfect) geometric image³⁵ of such a state on the phase plane is a static circle of the radius $A_n = x_0(2n + 1)^{1/2}$, along which the wavefunction is uniformly spread – see the blue rings in Fig. 8. For the ground state ($n = 0$), with the wavefunction (2.275), a better image may be a blurred round spot, of a radius $\sim x_0$, at the origin. (It is easy to criticize such blurring, intended to represent the non-vanishing spreads (99), because it fails to reflect the fact that the total energy of the oscillator in the state, $E_0 = \hbar\omega_0/2$ is definite, without any uncertainty.)

So, the difference between a classical state of the oscillator and its Fock state n is very profound; it is much similar to the difference between the classical picture of a freely moving 1D particle and the traveling de Broglie wave (1.88). However, the Fock states are not the only possible quantum states of the oscillator: according to the basic Eq. (4.6), any state described by the ket-vector

$$|\alpha\rangle = \sum_{n=0}^{\infty} \alpha_n |n\rangle \quad (5.105)$$

with an arbitrary set of (complex) c -numbers α_n , is also its legitimate state, subject only to the normalization condition $\langle \alpha | \alpha \rangle = 1$, giving

$$\sum_{n=0}^{\infty} |\alpha_n|^2 = 1. \quad (5.106)$$

³⁵ I have to confess that such geometric mapping of a quantum state onto the phase plane $[x, p]$ is not exactly defined; you may think about colored areas in Fig. 8 as the regions of the observable pairs $\{x, p\}$ most probably obtained in measurements. A quantitative definition of such a mapping will be given in Sec. 7.3 using the Wigner function, though, as we will see there, even such imaging has certain internal contradictions. Still, such cartoons as Fig. 8 have a substantial heuristic value, provided that their limitations are kept in mind.

It is natural to ask: could we select the coefficients α_n in such a special way that the state properties would be closer to the classical one; in particular the expectation values $\langle x \rangle$ and $\langle p \rangle$ of the coordinate and momentum would evolve in time as the classical values $X(t)$ and $P(t)$, while the uncertainties of these observables would be, just as in the ground state, given by Eqs. (99), and hence have the smallest possible uncertainty product, $\delta x \delta p = \hbar/2$. As early as 1926, E. Schrödinger showed that the answer was positive. In particular, by using special properties of the Hermite polynomials (2.281), he showed that the corresponding wavefunction, in the coordinate representation, is

$$\Psi_\alpha(x, t) = \left(\frac{m\omega_0}{\pi\hbar} \right)^{1/4} \exp \left\{ -\frac{m\omega_0}{2\hbar} [x - X(t)]^2 + i \frac{P(t)x}{\hbar} - i\phi(t) \right\}, \quad (5.107)$$

Glauber
state:
wavefunction

where

$$\phi(t) = \frac{\omega_0 t}{2} + \frac{X(t)P(t)}{2\hbar} + \text{const.} \quad (5.108)$$

This solution, whose validity may be readily verified by its substitution to the full Schrödinger equation for the oscillator's Hamiltonian (2.271) with the account of Eqs. (100), shows that such a *Glauber state*³⁶ is essentially the ground state but with its center shifted from the phase plane's origin to the classical oscillation point $\{X(t), P(t)\}$ – see the blurred red spot in Fig. 8. Moreover, it clearly shows that the coordinate's uncertainty, which is not affected by the x -independent phase shift $\phi(t)$, does not change with time, i.e. that in the harmonic oscillator, the Gaussian wave packet (107), once formed, does not spread with time. (As we have seen in Sec. 2.2, for a free particle, this is impossible.)

Moreover, a similar (though bulkier) calculation shows that the wavefunction (107), with the appropriately modified phase $\phi(t)$, also satisfies the Schrödinger equation of an oscillator under the effect of a pulse of a classical force $F(t)$, provided that the oscillator initially was in its ground state and that the classical evolution law $\{X(t), P(t)\}$ takes this force into account.³⁷ Since for many experimental implementations of the harmonic oscillator, the ground state may be readily formed (for example, by letting the oscillator relax via its weak coupling to a low-temperature environment), the Glauber state is usually easier to form than any Fock state with $n > 0$. This is why the Glauber states are so important and deserve a thorough discussion.

However, for such a discussion, the usual methods of wave mechanics and even the expansion (105) are rather inconvenient, because of the bulky coordinate representation (2.284) of the Fock states n . Instead, the needed calculations may be more readily done in the bra-ket formalism.

Let us start by expressing the double shift of the ground state (by X and by P), which is so evident in Eq. (107), in the operator language. Forgetting about the P for a minute, let us find the *translation operator* \hat{T}_X that would produce the desired shift of an arbitrary wavefunction $\psi(x)$ by a c -number distance X along the coordinate argument x . This means that

³⁶ Named after R. J. Glauber who studied these states in detail in the mid-1960s using operator methods – see below. Another popular adjective, “coherent”, for the Glauber states is very misleading, because *all* quantum states of *all* systems we have studied in this course so far, including the Fock states of the harmonic oscillator, may be represented as coherent (pure) superpositions of the basis states. This is why I will not use this term for the Glauber states.

³⁷ To find it, it is sufficient to integrate Eqs. (100) with $F(t)$ added to the right-hand side of the second of these equations. For their solution for an arbitrary $F(t)$, see, e.g., CM Eqs. (5.27) and (5.34) with $\delta = 0$.

$$\hat{\tau}_X \psi(x) \equiv \psi(x - X). \quad (5.109)$$

Representing the wavefunction ψ as the standard wave packet (4.264), we see that

$$\hat{\tau}_X \psi(x) = \frac{1}{(2\pi\hbar)^{1/2}} \int \varphi(p) \exp\left\{i \frac{p(x-X)}{\hbar}\right\} dp \equiv \frac{1}{(2\pi\hbar)^{1/2}} \int \left[\varphi(p) \exp\left\{-i \frac{pX}{\hbar}\right\} \right] \exp\left\{i \frac{px}{\hbar}\right\} dp. \quad (5.110)$$

Hence, the shift may be achieved by the multiplication of each Fourier component of the packet, with the momentum p , by $\exp\{-ipX/\hbar\}$. This gives us a hint that the general form of the translation operator, valid in *any* representation, should be

$$\hat{\tau}_X = \exp\left\{-i \frac{\hat{p}X}{\hbar}\right\}. \quad (5.111)$$

The proof of this formula is provided merely by the fact that, as we know from Chapter 4, any operator is uniquely determined by the set of its matrix elements in any full and orthogonal basis, in particular, the basis of the momentum states p . According to Eq. (110), the analog of Eq. (4.235) for the p -representation, applied to the translation operator (which is evidently local), is

$$\int dp \langle p | \hat{\tau}_X | p' \rangle \varphi(p') = \exp\left\{-i \frac{pX}{\hbar}\right\} \varphi(p), \quad (5.112)$$

so the operator (111) does exactly the job we need it to.

The operator that provides the shift of momentum by a c -number P is absolutely similar in structure – with the opposite sign under the exponent, due to the opposite sign of the exponent in the reciprocal Fourier transform, so the simultaneous shift by both X and P may be achieved by the following translation operator:

Translation
operator

$$\hat{\tau}_\alpha = \exp\left\{i \frac{P\hat{x} - \hat{p}X}{\hbar}\right\}. \quad (5.113)$$

As we already know, for a harmonic oscillator, the creation-annihilation operators are more natural, so we may use Eqs. (66) to recast Eq. (113) as

$$\hat{\tau}_\alpha = \exp\left\{\alpha \hat{a}^\dagger - \alpha^* \hat{a}\right\}, \quad \text{so } \hat{\tau}_\alpha^\dagger = \exp\left\{\alpha^* \hat{a} - \alpha \hat{a}^\dagger\right\}, \quad (5.114)$$

where α (which, generally, may be a function of time) is the c -number defined by Eq. (101). Now, getting clues from Eq. (107), we may form the Glauber state's ket-vector just as

$$|\alpha\rangle = \hat{\tau}_\alpha |0\rangle. \quad (5.115)$$

This formula, valid in any representation, is very elegant, but using it for practical calculations (say, of the expectation values of observables) is not too easy because of the exponent-of-operators form of the translation operator (113). Fortunately, it turns out that a much simpler representation of the Glauber state is possible. To show this, let us start with the following general (and very useful) property of exponential functions of an operator argument: if

$$[\hat{A}, \hat{B}] = \mu \hat{I}, \quad (5.116)$$

(where \hat{A} and \hat{B} are arbitrary linear operators, and μ is a c -number), then

$$\exp\{+\hat{A}\}\hat{B}\exp\{-\hat{A}\} = \hat{B} + \mu\hat{I}. \quad (5.117)$$

This relation may be readily proved by expanding the operator $\hat{f}(\lambda) \equiv \exp\{+\lambda\hat{A}\}\hat{B}\exp\{-\lambda\hat{A}\}$ in the Taylor series with respect to the c -number parameter λ , and then evaluating the result for $\lambda = 1$. (This simple exercise is left for the reader.)

Let us apply Eqs. (116)-(117) to two cases, both with

$$\hat{A} = \alpha^* \hat{a} - \alpha \hat{a}^\dagger, \quad \text{so} \quad \exp\{+\hat{A}\} = \hat{\tau}_\alpha^\dagger, \quad \exp\{-\hat{A}\} = \hat{\tau}_\alpha. \quad (5.118)$$

First, let us take $\hat{B} = \hat{I}$; then Eq. (116) is valid with $\mu = 0$, and Eq. (117) yields

$$\hat{\tau}_\alpha^\dagger \hat{\tau}_\alpha = \hat{I}, \quad (5.119)$$

This equality means that the translation operator is unitary – not a big surprise, because if we shift a classical point on the phase plane by a complex number $(+\alpha)$ and then by $(-\alpha)$, we certainly must come back to the initial position. Eq. (119) means merely that this fact is true for any quantum state as well.

Second, let us take $\hat{B} = \hat{a}$; in order to find the corresponding parameter μ , we must calculate the commutator on the left-hand side of Eq. (116) for this case. By using, at the due step of the calculation, Eq. (68), we get

$$[\hat{A}, \hat{B}] = [\alpha^* \hat{a} - \alpha \hat{a}^\dagger, \hat{a}] = -\alpha [\hat{a}^\dagger, \hat{a}] = \alpha \hat{I}, \quad (5.120)$$

so in this case $\mu = \alpha$, and Eq. (117) yields

$$\hat{\tau}_\alpha^\dagger \hat{a} \hat{\tau}_\alpha = \hat{a} + \alpha \hat{I}. \quad (5.121)$$

We have approached the summit of this beautiful calculation. Let us consider the following operator:

$$\hat{\tau}_\alpha \hat{\tau}_\alpha^\dagger \hat{a} \hat{\tau}_\alpha. \quad (5.122)$$

Using Eq. (119), we may reduce this product to $\hat{a} \hat{\tau}_\alpha$, while the application of Eq. (121) to the same expression (122) yields $\hat{\tau}_\alpha \hat{a} + \alpha \hat{\tau}_\alpha$. Hence, we get the following operator equality:

$$\hat{a} \hat{\tau}_\alpha = \hat{\tau}_\alpha \hat{a} + \alpha \hat{\tau}_\alpha, \quad (5.123)$$

which may be applied to any state. Now acting by both sides on the ground state's ket $|0\rangle$, and using the fact that $\hat{a}|0\rangle$ is the null state (while per Eq. (115), $\hat{\tau}_\alpha|0\rangle \equiv |\alpha\rangle$), we finally get a very simple and elegant result:³⁸

$$\hat{a}|\alpha\rangle = \alpha|\alpha\rangle. \quad (5.124)$$

Glauber
state as
eigenstate

³⁸ This result is also somewhat counterintuitive. Indeed, according to Eq. (89), the annihilation operator \hat{a} , acting upon a Fock state n , “beats it down” to the lower-energy state $(n - 1)$. However, according to Eq. (124), the action of the same operator on a Glauber state α does *not* lead to the state change and hence to any energy change! The resolution of this paradox is given by the representation of the Glauber state as a series of Fock states – see Eq. (134) below. The operator \hat{a} indeed transfers each Fock component of this series to a lower-energy state, but it also re-weights each term of the series, so the complete energy of the Glauber state remains constant.

Thus any Glauber state α is one of the eigenstates of the annihilation operator, namely the one with the eigenvalue equal to the c -number parameter α of the state, i.e. to the complex representation (101) of the classical point which is the center of the Glauber state's wavefunction.³⁹ This fact makes the calculations of all Glauber state properties much simpler. As an example, let us calculate $\langle x \rangle$ in the Glauber state with some c -number α :

$$\langle x \rangle = \langle \alpha | \hat{x} | \alpha \rangle = \frac{x_0}{\sqrt{2}} \langle \alpha | (\hat{a} + \hat{a}^\dagger) | \alpha \rangle \equiv \frac{x_0}{\sqrt{2}} \left(\langle \alpha | \hat{a} | \alpha \rangle + \langle \alpha | \hat{a}^\dagger | \alpha \rangle \right). \quad (5.125)$$

In the first term in the parentheses, we can apply Eq. (124) directly, while in the second term, we can use the bra-counterpart of that relation, $\langle \alpha | \hat{a}^\dagger = \langle \alpha | \alpha^*$. Now assuming that the Glauber state is normalized, $\langle \alpha | \alpha \rangle = 1$, and using Eq. (101), we get

$$\langle x \rangle = \frac{x_0}{\sqrt{2}} \left(\langle \alpha | \alpha | \alpha \rangle + \langle \alpha | \dots \alpha^* | \alpha \rangle \right) = \frac{x_0}{\sqrt{2}} (\alpha + \alpha^*) = X, \quad (5.126)$$

Acting absolutely similarly, we may verify that $\langle p \rangle = P$, and that δx and δp do indeed obey Eqs. (99), i.e. do not depend on the shift α . (This simple exercise is highly recommended to the reader.)

As the last sanity check, let us use Eq. (124) to re-calculate the Glauber state's wavefunction (107). Inner-multiplying both sides of that relation by the bra-vector $\langle x |$, and using the definition (65a) of the annihilation operator, we get

$$\frac{1}{\sqrt{2}x_0} \langle x | \left(\hat{x} + i \frac{\hat{p}}{m\omega_0} \right) | \alpha \rangle = \alpha \langle x | \alpha \rangle. \quad (5.127)$$

Since $\langle x |$ is the bra-vector of the eigenstate of the Hermitian operator \hat{x} , they may be swapped, with the operator giving its eigenvalue x ; acting on that bra-vector by the (local!) operator of momentum, we have to use it in the coordinate representation – see Eq. (4.245). As a result, we get

$$\frac{1}{\sqrt{2}x_0} \left(x \langle x | \alpha \rangle + \frac{\hbar}{m\omega_0} \frac{\partial}{\partial x} \langle x | \alpha \rangle \right) = \alpha \langle x | \alpha \rangle. \quad (5.128)$$

But $\langle x | \alpha \rangle$ is nothing else than the Glauber state's wavefunction Ψ_α , so Eq. (128) gives a first-order differential equation:

$$\frac{1}{\sqrt{2}x_0} \left(x \Psi_\alpha + \frac{\hbar}{m\omega_0} \frac{\partial}{\partial x} \Psi_\alpha \right) = \alpha \Psi_\alpha. \quad (5.129)$$

Chasing Ψ_α and x to the opposite sides of the equation, and using the definition (101) of the parameter α , we can bring this equation to the following form:

$$\frac{\partial \Psi_\alpha}{\Psi_\alpha} = \frac{m\omega_0}{\hbar} \left[-x + \left(X + i \frac{P}{m\omega_0} \right) \right] \partial x. \quad (5.130)$$

Integrating both parts (over x only!), we return to Eq. (107).

³⁹ This fact means that the spectrum of eigenvalues α in Eq. (124), viewed as an eigenproblem, is continuous – it may be *any* complex number.

Now we can use Eq. (124) for finding the coefficients α_n in the expansion (105) of the Glauber state α in the series over the Fock states n . Plugging Eq. (105) into both sides of Eq. (124), using the second of Eqs. (89) on the left-hand side, and requiring the coefficients at each ket-vector $|n\rangle$ in both parts of the resulting relation to be equal, we get the following recurrence relation:

$$\alpha_{n+1} = \frac{\alpha}{(n+1)^{1/2}} \alpha_n. \tag{5.131}$$

Applying this relation sequentially for $n = 0, 1, 2$, etc., we get

$$\alpha_n = \frac{\alpha^n}{(n!)^{1/2}} \alpha_0. \tag{5.132}$$

Now we can find α_0 from the normalization requirement (106), getting

$$|\alpha_0|^2 \sum_{n=0}^{\infty} \frac{|\alpha|^{2n}}{n!} = 1. \tag{5.133}$$

In this sum, we may readily recognize the Taylor expansion of the function $\exp\{|\alpha|^2\}$, so the final result (besides an arbitrary common phase multiplier) is

$$|\alpha\rangle = \exp\left\{-\frac{|\alpha|^2}{2}\right\} \sum_{n=0}^{\infty} \frac{\alpha^n}{(n!)^{1/2}} |n\rangle. \tag{5.134}$$

Glauber state vs Fock states

Hence, if the oscillator is in the Glauber state α , the probabilities $W_n \equiv \alpha_n \alpha_n^*$ of finding the system on the n^{th} energy level (86) obey the well-known *Poisson distribution* (Fig. 9):

$$W_n = \frac{\langle n \rangle^n}{n!} e^{-\langle n \rangle}, \tag{5.135}$$

Poisson distribution

where $\langle n \rangle$ is the statistical average of n – see Eq. (1.37):

$$\langle n \rangle = \sum_{n=0}^{\infty} n W_n. \tag{5.136}$$

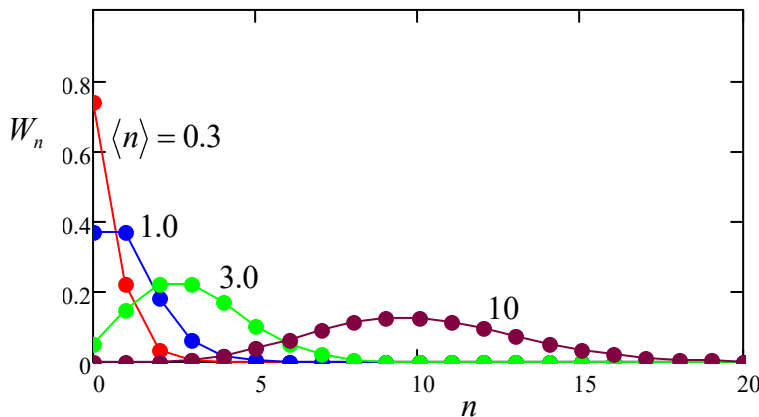


Fig. 5.9. The Poisson distribution (135) for several values of $\langle n \rangle$. Note that W_n are defined only for integer values of n , so the lines are only guides for the eye.

Note that the result of such summation is not necessarily an integer; in our particular case,

$$\langle n \rangle = |\alpha|^2. \quad (5.137)$$

For applications, perhaps the most important property of this distribution is that for any $\langle n \rangle$,

$$\langle \tilde{n}^2 \rangle \equiv \langle (n - \langle n \rangle)^2 \rangle = \langle n \rangle, \quad \text{so that } \delta n \equiv \langle \tilde{n}^2 \rangle^{1/2} = \langle n \rangle^{1/2}. \quad (5.138)$$

Glauber state:
r.m.s.
uncertainty

Another important property is that at $\langle n \rangle \gg 1$, the Poisson distribution approaches the Gaussian one, with W_n peaking at $n = \langle n \rangle = |\alpha|^2$, and a small relative r.m.s. uncertainty: $\delta n / \langle n \rangle \ll 1$ – see Fig. 9.

Now let us discuss the Glauber state's evolution in time. In the wave-mechanics language, it is completely described by the dynamics (100) of the c -number shifts $X(t)$ and $P(t)$ participating in the wavefunction (107). An alternative and equivalent way of dynamics description is to use the Heisenberg equation of motion. As Eqs. (29) and (35) tell us, such equations for the Heisenberg operators of coordinate and momentum have to be similar to the classical equations (100):

$$\dot{\hat{x}}_H = \frac{\hat{p}_H}{m}, \quad \dot{\hat{p}}_H = -m\omega_0^2 \hat{x}_H. \quad (5.139)$$

Now using Eqs. (66), for the Heisenberg-picture creation and annihilation operators we get the equations

$$\dot{\hat{a}}_H = -i\omega_0 \hat{a}_H, \quad \dot{\hat{a}}_H^\dagger = +i\omega_0 \hat{a}_H^\dagger, \quad (5.140)$$

which are completely similar to the classical equation (102) for the c -number parameter α and its complex conjugate, and hence have the solutions identical to Eq. (103):

$$\hat{a}_H(t) = \hat{a}_H(0)e^{-i\omega_0 t}, \quad \hat{a}_H^\dagger(t) = \hat{a}_H^\dagger(0)e^{i\omega_0 t}. \quad (5.141)$$

As was discussed in Sec. 4.6, such equations are very convenient because they enable simple calculation of time evolution of observables for any initial state of the oscillator (Fock, Glauber, or any other) by using Eq. (4.191). In particular, Eq. (141), without any calculations, shows that regardless of its initial state, the oscillator always returns to it *exactly* with the period $2\pi/\omega_0$.⁴⁰

Applied to the particular case of the ground state of the oscillator, Eq. (141) confirms that the Gaussian wave packet of the special width (99) does not spread in time at all – even temporarily. At this point, I have to notice that there exist other ground-like states whose initial wave packets are still Gaussian but have different widths, say $\delta x < x_0/\sqrt{2}$. As we already know from Sec. 2.2, the momentum spread δp has to be correspondingly larger, but the uncertainty product may still be the smallest: $\delta x \delta p = \hbar/2$. Such *squeezed ground states* ζ , with zero expectation values of x and p , may be generated from the Fock/Glauber ground state:

$$|\zeta\rangle = \hat{S}_\zeta |0\rangle, \quad (5.142a)$$

Squeezed
ground
state

by using the so-called *squeezing operator*:

⁴⁰ Actually, this fact is also evident from the Schrödinger picture of the oscillator's time evolution: due to the exactly equal distances $\hbar\omega_0$ between the eigenenergies (86), the time functions $a_n(t)$ in the fundamental expansion (1.69) of its wavefunction oscillate with frequencies $n\omega_0$, and hence they all share the basic time period $2\pi/\omega_0$.

$$\hat{S}_\zeta \equiv \exp\left\{\frac{1}{2}\left(\zeta^* \hat{a}\hat{a} - \zeta \hat{a}^\dagger \hat{a}^\dagger\right)\right\}, \quad (5.142b) \quad \text{Squeezing operator}$$

which depends on the complex c -number parameter $\zeta = r e^{i\theta}$, where r and θ are real. The parameter's modulus r determines the squeezing degree; if ζ is real (i.e. $\theta = 0$), then

$$\delta x = \frac{x_0}{\sqrt{2}} e^{-r}, \quad \delta p = \frac{m\omega_0 x_0}{\sqrt{2}} e^r, \quad \text{so } \delta x \delta p = \frac{m\omega_0 x_0^2}{2} \equiv \frac{\hbar}{2}. \quad (5.143)$$

On the phase plane (Fig. 8), this state, with $r > 0$, may be represented by an oval spot squeezed along one of two mutually perpendicular axes (hence the state's name), and stretched by the same factor e^r along the counterpart axis; the same formulas but with $r < 0$ describe squeezing along the other axis. On the other hand, the phase θ of the squeezing parameter ζ determines the angle $\theta/2$ of the squeezing/stretching axes about the phase plane origin – see the magenta ellipse in Fig. 8. If $\theta \neq 0$, Eqs. (143) are valid for the variables $\{x', p'\}$ obtained from $\{x, p\}$ via clockwise rotation by that angle. For any of such origin-centered squeezed ground states, the time evolution is reduced to an increase of the angle with the rate ω_0 , i.e. to the clockwise rotation of the ellipse, without its deformation, with the angular velocity ω_0 – see the magenta arrows in Fig. 8. As a result, the uncertainties δx and δp oscillate in time with the double frequency $2\omega_0$. Such squeezed ground states may be formed, for example, by a parametric excitation of the oscillator,⁴¹ with a parameter modulation depth close to, but still below the threshold of the excitation of degenerate parametric oscillations.

By action of an additional external force (or by appropriate initial state preparation), the center of a squeezed state may be displaced from the origin to an arbitrary point $\{X, P\}$. Such a displaced squeezed state may be described by the action of the translation operator (113) upon the ground squeezed state, i.e. by the action of the operator product $\hat{T}_\alpha \hat{S}_\zeta$ on the usual (Fock/Glauber, i.e. non-squeezed) ground state. Calculations similar to those that led us from Eq. (114) to Eq. (124), show that the displaced squeezed state is an eigenstate of the following mixed operator:

$$\hat{b} \equiv \hat{a} \cosh r + \hat{a}^\dagger e^{i\theta} \sinh r, \quad (5.144)$$

with the same parameters r and θ , with the eigenvalue

$$\beta = \alpha \cosh r + \alpha^* e^{i\theta} \sinh r, \quad (5.145)$$

thus generalizing Eq. (124), which corresponds to $r = 0$. For the particular case $\alpha = 0$, Eq. (145) yields $\beta = 0$, i.e. the action of the operator (144) on the squeezed ground state ζ yields the null state. Just as Eq. (124) in the case of the Glauber states, Eqs. (144)-(145) make the calculation of the basic properties of the squeezed states (for example, the proof of Eqs. (143) for the case $\alpha = \theta = 0$) very straightforward.

Unfortunately, I do not have more time/space for a further discussion of the squeezed states in this chapter (besides a few problems given for the reader's exercise), but their importance for precise quantum measurements will be discussed in Sec. 10.2 below.⁴²

⁴¹ For a discussion and classical theory of this effect, see, e.g., CM Sec. 5.5.

⁴² For more on the squeezed states see, e.g., Chapter 7 in the monograph by C. Gerry and P. Knight, *Introductory Quantum Optics*, Cambridge U. Press, 2005. Also, note the spectacular measurements of the Glauber and squeezed states of electromagnetic (optical) oscillators by G. Breitenbach *et al.*, *Nature* **387**, 471 (1997), a large

5.6. Orbital angular momentum

One more blank spot to fill has been left by our study, in Sec. 3.6, of wave mechanics of particle motion in spherically symmetric 3D potentials. Indeed, while the azimuthal components of the eigenfunctions (the spherical harmonics) of such systems are very simple,

$$\psi_m = (2\pi)^{-1/2} e^{im\varphi}, \quad \text{with } m = 0, \pm 1, \pm 2, \dots, \quad (5.146)$$

their polar components include the associated Legendre functions $P_l^m(\cos\theta)$, which may be expressed via elementary functions only indirectly – see Eqs. (3.165) and (3.168). This makes all the calculations less than transparent and, in particular, does not allow a clear insight into the origin of the very simple energy spectrum of such systems – see, e.g., Eq. (3.163). The bra-ket formalism, applied to the angular momentum operator, not only enables such insight and produces a very convenient tool for many calculations involving spherically symmetric potentials but also opens a clear way toward the unification of the orbital momentum with the particle's spin – the latter task to be addressed in the next section.

Let us start by using the correspondence principle to spell out the quantum-mechanical vector operator of the orbital angular momentum $\mathbf{L} \equiv \mathbf{r} \times \mathbf{p}$ of a point particle:

Angular
momentum
operator

$$\hat{\mathbf{L}} \equiv \hat{\mathbf{r}} \times \hat{\mathbf{p}} = \begin{vmatrix} \mathbf{n}_x & \mathbf{n}_y & \mathbf{n}_z \\ \hat{r}_1 & \hat{r}_2 & \hat{r}_3 \\ \hat{p}_1 & \hat{p}_2 & \hat{p}_3 \end{vmatrix}, \quad \text{i.e. } \hat{L}_j \equiv \sum_{j', j''=1}^3 \hat{r}_{j'} \hat{p}_{j''} \varepsilon_{jj'j''}, \quad (5.147)$$

where $\varepsilon_{jj'j''}$ is the Levi-Civita permutation symbol, which we have already used in Sec. 4.5, and also in Sec. 1 of this chapter in similar expressions (17)-(18). From this definition, we can readily calculate the commutation relations for all Cartesian components of the vector operators of \mathbf{L} , \mathbf{r} , and \mathbf{p} , for example,

$$[\hat{L}_j, \hat{r}_{j'}] = \left[\sum_{k, j''=1}^3 \hat{r}_k \hat{p}_{j''} \varepsilon_{jkj''}, \hat{r}_{j'} \right] \equiv - \sum_{k, j''=1}^3 \hat{r}_k [\hat{r}_{j'}, \hat{p}_{j''}] \varepsilon_{jkj''} = -i\hbar \sum_{k, j''=1}^3 \hat{r}_k \delta_{jj''} \varepsilon_{jkj''} = i\hbar \sum_{j''=1}^3 \hat{r}_{j''} \varepsilon_{jjj''}. \quad (5.148)$$

The summary of all these calculations may be represented in similar forms:

Key
commutation
relations

$$[\hat{L}_j, \hat{r}_{j'}] = i\hbar \sum_{j''=1}^3 \hat{r}_{j''} \varepsilon_{jjj''}, \quad [\hat{L}_j, \hat{p}_{j'}] = i\hbar \sum_{j''=1}^3 \hat{p}_{j''} \varepsilon_{jjj''}, \quad [\hat{L}_j, \hat{L}_{j'}] = i\hbar \sum_{j''=1}^3 \hat{L}_{j''} \varepsilon_{jjj''}; \quad (5.149)$$

the last of them shows that the commutator of two different Cartesian components of $\hat{\mathbf{L}}$ is proportional to its complementary component.

Also introducing, in a natural way, the (scalar!) operator of the observable $L^2 \equiv |\mathbf{L}|^2$,

Operator
of L^2

$$\hat{L}^2 \equiv \hat{L}_x^2 + \hat{L}_y^2 + \hat{L}_z^2 \equiv \sum_{j=1}^3 \hat{L}_j^2, \quad (5.150)$$

it is straightforward to check that this operator commutes with each of the Cartesian components:

(ten-fold) squeezing achieved in such oscillators by H. Vahlbruch *et al.*, *Phys. Rev. Lett.* **100**, 033602 (2008), and the first results on the ground state squeezing in micromechanical oscillators, with resonance frequencies $\omega_0/2\pi$ as low as a few MHz, by using their parametric coupling to microwave electromagnetic oscillators – see, e.g., E. Wollman *et al.*, *Science* **349**, 952 (2015) and/or J.-M. Pirkkalainen *et al.*, *Phys. Rev. Lett.* **115**, 243601 (2015).

$$[\hat{L}^2, \hat{L}_j] = 0. \quad (5.151)$$

This result, at first sight, may seem to contradict the last of Eqs. (149). Indeed, haven't we learned in Sec. 4.5 that commuting operators (e.g., \hat{L}^2 and any of \hat{L}_j) share their eigenstate sets? If yes, shouldn't this set has to be common for all four angular momentum operators? The resolution in this paradox may be found in the condition that was mentioned just after Eq. (4.138), but (sorry!) was not sufficiently emphasized there. According to that relation, if an operator has *degenerate* eigenstates (i.e. if some $A_j = A_{j'}$, even for $j \neq j'$), they should not be necessarily all shared by another compatible operator.

This is exactly the situation with the orbital angular momentum operators, which may be schematically represented by the *Venn diagram*⁴³ shown in Fig. 10: the eigenstates of the operator \hat{L}^2 are highly degenerate,⁴⁴ and their set is broader than those of any component operator \hat{L}_j (that, as will be shown below, are non-degenerate – until we consider the particle's spin).

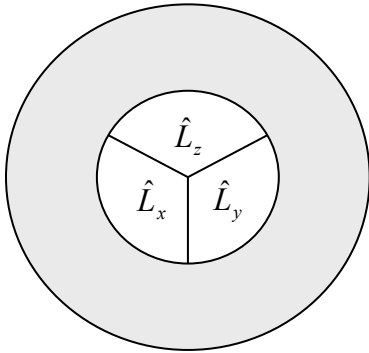


Fig. 5.10. The Venn diagram showing the partitioning of the set of eigenstates of the operator \hat{L}^2 . Each inner sector corresponds to the states shared with one of the Cartesian component operators \hat{L}_j , while the outer (shaded) ring represents the eigenstates of \hat{L}^2 that are not shared with either of \hat{L}_j – for example, all linear combinations of the eigenstates of different component operators.

Let us focus on just one of these three joint sets of eigenstates – by tradition, of the operators \hat{L}^2 and \hat{L}_z . (This tradition stems from the canonical form of the spherical coordinates, in which the polar angle is measured from the z-axis. Indeed, in the coordinate representation, we may write

$$\hat{L}_z \equiv \hat{x}p_y - \hat{y}p_x = x \left(-i\hbar \frac{\partial}{\partial y} \right) - y \left(-i\hbar \frac{\partial}{\partial x} \right) = -i\hbar \frac{\partial}{\partial \varphi}. \quad (5.152)$$

Writing the standard eigenproblem for the operator in this representation, $\hat{L}_z \psi_m = L_z \psi_m$, we see that it is satisfied by the eigenfunctions (146), with eigenvalues $L_z = \hbar m$ – the fact that was already conjectured in Sec. 3.5.) More specifically, let us consider a set of eigenstates $\{l, m\}$ corresponding to a certain degenerate eigenvalue of the operator \hat{L}^2 , and all possible eigenvalues of the operator \hat{L}_z , i.e. all possible quantum numbers m . (At this point, l is just a label of the eigenvalue of the operator \hat{L}^2 ; it will

⁴³ This is just a particular example of the Venn diagrams (introduced in the 1880s by John Venn) that show possible relations (such as intersections, unions, complements, etc.) between various sets of objects, and are a very useful notion of the general set theory.

⁴⁴ Note that this particular result is consistent with the classical picture of the angular momentum vector: even when its length is fixed, the vector may be oriented in various directions, corresponding to different values of its Cartesian components. However, in the classical picture, all these components may have exactly fixed values simultaneously, while in the quantum picture, this is not true.

be defined more explicitly in a minute.) To analyze this set, it is instrumental to introduce the so-called *ladder* (also called, respectively, “raising” and “lowering”) *operators*⁴⁵

Ladder operators

$$\hat{L}_{\pm} \equiv \hat{L}_x \pm i\hat{L}_y. \tag{5.153}$$

It is simple (and hence left for the reader’s exercise) to use this definition and the last of Eqs. (149) to calculate the following commutators:

Important commutation relations

$$[\hat{L}_+, \hat{L}_-] = 2\hbar\hat{L}_z, \quad \text{and} \quad [\hat{L}_z, \hat{L}_{\pm}] = \pm\hbar\hat{L}_{\pm}, \tag{5.154}$$

and also to use Eqs. (149)-(150) to prove two other important operator relations:

$$\hat{L}^2 = \hat{L}_z^2 + \hat{L}_+ \hat{L}_- - \hbar\hat{L}_z, \quad \hat{L}^2 = \hat{L}_z^2 + \hat{L}_- \hat{L}_+ + \hbar\hat{L}_z. \tag{5.155}$$

Now let us rewrite the last of Eqs. (154) as

$$\hat{L}_z \hat{L}_{\pm} = \hat{L}_{\pm} \hat{L}_z \pm \hbar\hat{L}_{\pm}, \tag{5.156}$$

and act by both its sides upon the ket-vector $|l, m\rangle$ of an arbitrary common eigenstate:

$$\hat{L}_z \hat{L}_{\pm} |l, m\rangle = \hat{L}_{\pm} \hat{L}_z |l, m\rangle \pm \hbar\hat{L}_{\pm} |l, m\rangle. \tag{5.157}$$

Since the eigenvalues of the operator \hat{L}_z are equal to $\hbar m$, in the first term of the right-hand side of Eq. (157) we may write

$$\hat{L}_z |l, m\rangle = \hbar m |l, m\rangle. \tag{5.158}$$

With that, Eq. (157) may be recast as

$$\hat{L}_z (\hat{L}_{\pm} |l, m\rangle) = \hbar(m \pm 1) (\hat{L}_{\pm} |l, m\rangle). \tag{5.159}$$

In a spectacular similarity with Eqs. (78)-(79) for the harmonic oscillator, Eq. (159) means that the states $\hat{L}_{\pm} |l, m\rangle$ are also eigenstates of the operator \hat{L}_z , corresponding to eigenvalues $\hbar(m \pm 1)$. Thus the ladder operators work exactly as the creation and annihilation operators of a harmonic oscillator, moving the system up or down a ladder of eigenstates – see Fig. 11.

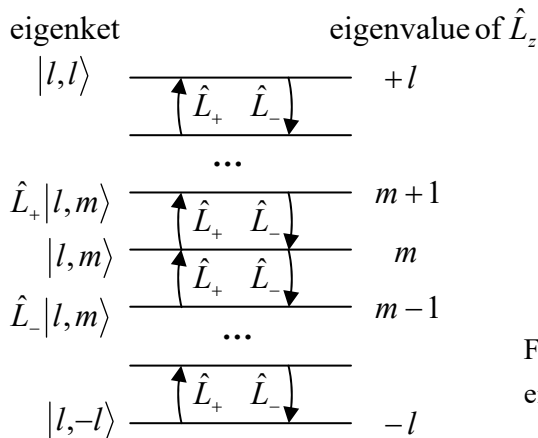


Fig. 5.11. The ladder diagram of the common eigenstates of the operators \hat{L}^2 and \hat{L}_z .

⁴⁵ Note a substantial similarity between this definition and Eqs. (65) for the creation/annihilation operators.

The most significant difference is that now the state ladder must end in both directions, because an infinite increase of $|m|$, with whichever sign of m , would cause the expectation values of the operator

$$\hat{L}_x^2 + \hat{L}_y^2 \equiv \hat{L}^2 - \hat{L}_z^2, \quad (5.160)$$

which corresponds to a non-negative observable, becoming negative. Hence there have to be two states at both ends of the ladder, with such ket-vectors $|l, m_{\max}\rangle$ and $|l, m_{\min}\rangle$ that

$$\hat{L}_+ |l, m_{\max}\rangle = 0, \quad \hat{L}_- |l, m_{\min}\rangle = 0. \quad (5.161)$$

Due to the symmetry of the whole problem with respect to the replacement $m \rightarrow -m$, we should have $m_{\min} = -m_{\max}$. This m_{\max} is exactly the quantum number traditionally called l , i.e.

$$-l \leq m \leq +l. \quad (5.162)$$

Relation
between
 m and l

This relation of the quantum numbers m and l is semi-quantitatively compatible with the classical image of the angular momentum vector \mathbf{L} , of the same length L , pointing in various directions, thus affecting the value of its component L_z . In this classical picture, however, L^2 would be equal to the square of $(L_z)_{\max}$, i.e. to $(\hbar l)^2$; however, in quantum mechanics, this is not so. Indeed, applying both parts of the second of the operator equalities (155) to the top state's vector $|l, m_{\max}\rangle \equiv |l, l\rangle$, we get

$$\begin{aligned} \hat{L}^2 |l, l\rangle &= \hbar \hat{L}_z |l, l\rangle + \hat{L}_z^2 |l, l\rangle + \hat{L}_- \hat{L}_+ |l, l\rangle = \hbar^2 l |l, l\rangle + \hbar^2 l^2 |l, l\rangle + 0 \\ &\equiv \hbar^2 l(l+1) |l, l\rangle. \end{aligned} \quad (5.163)$$

Since by our initial assumption, all eigenvectors $|l, m\rangle$ correspond to the same eigenvalue of \hat{L}^2 , this result means that *all* these eigenvalues are equal to $\hbar^2 l(l+1)$. Just as in the case of the spin- $1/2$ vector operators discussed in Sec. 4.5, the deviation of this result from $\hbar^2 l^2$ may be interpreted as a result of unavoidable uncertainties (“fluctuations”) of the x - and y -components of the angular momentum, which give non-zero positive contributions to $\langle L_x^2 \rangle$ and $\langle L_y^2 \rangle$, and hence to $\langle L^2 \rangle$, even if the angular momentum vector is aligned with the z -axis in the best possible way.⁴⁶

(For applications, one more relation, in one of its two equivalent forms, may be convenient:

$$\hat{L}_\pm |l, m\rangle = \hbar [l(l+1) - m(m \pm 1)]^{1/2} |l, m \pm 1\rangle \equiv \hbar [(l \pm m + 1)(l \mp m)]^{1/2} |l, m \pm 1\rangle. \quad (5.164)$$

This equality, valid to the multiplier $e^{i\varphi}$ with an arbitrary real phase φ , may be readily proved from the above relations in the same way as the parallel Eqs. (89) for the harmonic-oscillator operators (65) were proved in Sec. 4; due to this similarity, the proof is also left for the reader's exercise.⁴⁷)

⁴⁶ Curiously, a similar formula $\langle L^2 \rangle = \hbar^2 l(l+1)$ may be also obtained by assuming that all $(2l+1)$ values $L_z = \hbar m$ of a system with fixed l have equal probability. (Let me leave the proof for the reader's exercise.)

⁴⁷ The reader is also challenged to use the commutation relations discussed above to prove one more important property of the common eigenstates of the operators \hat{L}_z and \hat{L}^2 :

$$\langle l, m | \hat{r}_j | l', m' \rangle = 0, \quad \text{unless } l' = l \pm 1 \text{ and } m' = \text{either } m \pm 1 \text{ or } m.$$

This property gives the *selection rule* for the orbital electric-dipole quantum transitions, to be discussed later in the course, especially in Sec. 9.3. (The final selection rules at these transitions may be affected by the particle's spin – see the next section.)

Note that the formulas discussed in this section, with the sole exception of Eq. (146), are not conditioned by a particular Hamiltonian of the system under analysis. However, they (as well as those discussed in the next section) are especially important for particles moving in spherically-symmetric potentials, which were discussed in Sec. 3.6. It is easy (and hence is also left for the reader's exercise) to prove that in this case, the particle's Hamiltonian operator commutes with that of the angular momentum, so according to Eq. (4.199), in the Heisenberg picture of quantum dynamics, the Cartesian components \hat{L}_j as well as \hat{L}^2 do not depend on time, and hence their expectation values are integrals of motion.

By using the expression of Cartesian coordinates via the spherical ones exactly as this was done in Eq. (152), we get the following expressions for the ladder operators (153) in the coordinate representation:

$$\hat{L}_{\pm} = \hbar e^{\pm i\varphi} \left(\pm \frac{\partial}{\partial \theta} + i \cotan \theta \frac{\partial}{\partial \varphi} \right). \quad (5.165)$$

Now plugging this relation, together with Eq. (152), into any of Eqs. (155), we get

$$\hat{L}^2 = -\hbar^2 \left[\frac{1}{\sin \theta} \frac{\partial}{\partial \theta} \left(\sin \theta \frac{\partial}{\partial \theta} \right) + \frac{1}{\sin^2 \theta} \frac{\partial^2}{\partial \varphi^2} \right]. \quad (5.166)$$

But this is exactly the operator (besides its division by the constant parameter $2mR^2$) that stands on the left-hand side of Eq. (3.156). Hence that equation, which was explored by the “brute-force” (wave-mechanical) approach in Sec. 3.6, may be understood as the eigenproblem for the operator \hat{L}^2 in the coordinate representation, with the eigenfunctions $Y_l^m(\theta, \varphi)$ corresponding to the eigenkets $|l, m\rangle$, and the eigenvalues $L^2 = 2mR^2 E$. As a reminder, the main result of that, rather involved analysis was expressed by Eq. (3.163), which now may be rewritten as

$$L_l^2 \equiv 2mR^2 E_l = \hbar^2 l(l+1), \quad (5.167)$$

in full agreement with Eq. (163), which was obtained by much more efficient means based on the bracket formalism. In particular, it is fascinating to see how easy it is to operate with the eigenvectors $|l, m\rangle$, while the coordinate representations of these vectors, the spherical harmonics $Y_l^m(\theta, \varphi)$, may be only expressed by rather complicated functions – please have one more look at Eq. (3.171) and Fig. 3.20.

5.7. Spin and total angular momentum

The theory described in the last section is useful for much more than orbital motion analysis. In particular, it helps to generalize the spin- $1/2$ results discussed in Chapter 4 to other values of spin s – the parameter still to be quantitatively defined. For that, let us notice that the commutation relations (4.155) for spin- $1/2$, which were derived from the Pauli matrix properties, may be rewritten in exactly the same form as Eqs. (149) and (151) for the orbital momentum:

$$[\hat{S}_j, \hat{S}_{j'}] = i\hbar \sum_{j''=1}^3 \hat{S}_{j''} \varepsilon_{jjj''}, \quad [\hat{S}^2, \hat{S}_j] = 0. \quad (5.168)$$

It had been postulated (and then confirmed by numerous experiments) that these relations hold for quantum particles with any spin. Now notice that all the calculations of the last section have been based *almost* exclusively on such relations – the only exception will be discussed imminently. Hence, we may repeat them for the spin operators, and get the relations similar to Eqs. (158) and (163):

$$\hat{S}_z |s, m_s\rangle = \hbar m_s |s, m_s\rangle, \quad \hat{S}^2 |s, m_s\rangle = \hbar^2 s(s+1) |s, m_s\rangle, \quad 0 \leq s, \quad -s \leq m_s \leq +s, \quad (5.169)$$

Spin operators: eigenstates and eigenvalues

where m_s is a quantum number parallel to the orbital magnetic number m , and the non-negative constant s is defined as the maximum value of $|m_s|$. The c -number s is exactly what is called the *particle's spin*.

Now let us return to the only part of our orbital moment calculations that has *not* been derived from the commutation relations. This was the fact, based on the solution (146) of the orbital motion problems, that the quantum number m (the analog of m_s) may be only an integer. For spin, we do not have such a solution, so the spectrum of numbers m_s (and hence its limits $\pm s$) should be found from the more loose requirement that the eigenstate ladder, extending from $-s$ to $+s$, has an integer number of steps. Hence, $2s$ has to be an integer, i.e. the spin s of a quantum particle may be either *integer* (as it is, for example, for photons, gluons, and massive bosons W^\pm and Z^0), or *half-integer* (e.g., for all quarks and leptons, notably including electrons).⁴⁸ For $s = 1/2$, this picture yields all the properties of the spin- $1/2$ that were derived in Chapter 4 from Eqs. (4.115)-(4.117). In particular, the operators \hat{S}^2 and \hat{S}_z have two common eigenstates (\uparrow and \downarrow), with $S_z = \hbar m_s = \pm \hbar/2$, both with $S^2 = s(s+1)\hbar^2 = (3/4)\hbar^2$.

Note that this analogy with the angular momentum sheds new light on the symmetry properties of spin- $1/2$. Indeed, the fact that m in Eq. (146) is an integer was derived in Sec. 3.5 from the requirement that making a full circle around the z -axis, we should find a similar final value of the wavefunction ψ_m , which may differ from the initial one only by an inconsequential factor $\exp\{2\pi i m\} = +1$. With the replacement $m \rightarrow m_s = \pm 1/2$, such an operation would multiply the wavefunction by $\exp\{\pm \pi i\} = -1$, i.e. reverse its sign. Of course, spin properties cannot be described by a usual wavefunction, but this *odd parity* of electrons, shared by all other spin- $1/2$ particles, is clearly revealed in properties of multiparticle systems (see Chapter 8 below), and as a result, in their statistics (see, e.g., SM Chapter 2).

Now we are sufficiently equipped to analyze the situations in which a particle has both the orbital momentum and the spin – as an electron inside an atom. In classical mechanics, such an object, with the spin \mathbf{S} interpreted as the angular moment of its internal rotation, would be characterized by the *total angular momentum* vector $\mathbf{J} = \mathbf{L} + \mathbf{S}$. Following the correspondence principle, we may assume that quantum-mechanical properties of this observable may be described by the similarly defined vector operator:

$$\hat{\mathbf{J}} \equiv \hat{\mathbf{L}} + \hat{\mathbf{S}}, \quad (5.170)$$

Total angular momentum

with Cartesian components

$$\hat{J}_z \equiv \hat{L}_z + \hat{S}_z, \text{ etc.}, \quad (5.171)$$

and the magnitude squared equal to

$$\hat{J}^2 \equiv \hat{J}_x^2 + \hat{J}_y^2 + \hat{J}_z^2. \quad (5.172)$$

⁴⁸ As a reminder, in the Standard Model of particle physics, such hadrons as mesons and baryons (notably including protons and neutrons) are essentially composite particles. However, at non-relativistic energies, protons and neutrons may be considered fundamental particles with $s = 1/2$.

Let us examine the key properties of this vector operator. Since its two components (170) describe different degrees of freedom of the particle, i.e. belong to different Hilbert spaces, they have to be completely commuting:

$$[\hat{L}_j, \hat{S}_{j'}] = 0, \quad [\hat{L}^2, \hat{S}^2] = 0, \quad [\hat{L}_j, \hat{S}^2] = 0, \quad [\hat{L}^2, \hat{S}_j] = 0. \quad (5.173)$$

The above formulas are sufficient to derive the commutation relations for the operator $\hat{\mathbf{J}}$, and unsurprisingly, they turn out to be absolutely similar to those of its orbital and spin components:

Total
momentum:
commutation
relations

$$[\hat{J}_j, \hat{J}_{j'}] = i\hbar \sum_{j''=1}^3 \hat{J}_{j''} \varepsilon_{jjj''}, \quad [\hat{J}^2, \hat{J}_j] = 0. \quad (5.174)$$

Now by repeating all the arguments of the last section, we may derive the following expressions for the common eigenstates of the operators \hat{J}^2 and \hat{J}_z :

Total
momentum:
eigenstates,
and
eigenvalues

$$\hat{J}_z |j, m_j\rangle = \hbar m_j |j, m_j\rangle, \quad \hat{J}^2 |j, m_j\rangle = \hbar^2 j(j+1) |j, m_j\rangle, \quad 0 \leq j, \quad -j \leq m_j \leq +j, \quad (5.175)$$

where j and m_j are new quantum numbers.⁴⁹ Repeating the arguments just made for s and m_s , we may conclude that j and m_j may be either integers or half-integers.

Before we proceed, one remark on notation: it is very convenient to use the same letter m for numbering eigenstates of all momentum components participating in Eq. (171), with corresponding indices (j , l , and s), in particular, to replace what we called m with m_l . With this replacement, the main results of the last section may be summarized in a form similar to Eqs. (168), (169), (174), and (175):

$$[\hat{L}_j, \hat{L}_{j'}] = i\hbar \sum_{j''=1}^3 \hat{L}_{j''} \varepsilon_{jjj''}, \quad [\hat{L}^2, \hat{L}_j] = 0, \quad (5.176)$$

Orbital
momentum:
basic
properties
(new notation)

$$\hat{L}_z |l, m_l\rangle = \hbar m_l |l, m_l\rangle, \quad \hat{L}^2 |l, m_l\rangle = \hbar^2 l(l+1) |l, m_l\rangle, \quad 0 \leq l, \quad -l \leq m_l \leq +l. \quad (5.177)$$

In order to understand which eigenstates participating in Eqs. (169), (175), and (177) are compatible with each other, it is straightforward to use Eq. (172), together with Eqs. (168), (173), (174), and (176) to get the following relations:

$$[\hat{J}^2, \hat{L}^2] = 0, \quad [\hat{J}^2, \hat{S}^2] = 0, \quad (5.178)$$

$$[\hat{J}^2, \hat{L}_z] \neq 0, \quad [\hat{J}^2, \hat{S}_z] \neq 0. \quad (5.179)$$

This result is represented schematically on the Venn diagram shown in Fig. 12, in which the crossed arrows indicate the only *non*-commuting pairs of operators. The color lines in this figure encircle two operator groups that commute with each other and hence may share their eigenstates. The first group (encircled red), consists of all operators but \hat{J}^2 ; their shared eigenstates correspond to definite values of the corresponding quantum numbers: l , m_l , s , m_s , and m_j . Actually, only four of these numbers are independent, because due to Eq. (171) for these compatible operators, for each eigenstate of this group, their “magnetic” quantum numbers m have to satisfy the following relation:

⁴⁹ Let me hope that the difference between the quantum number j , and the indices j, j', j'' numbering the Cartesian components in relations like Eqs. (168) or (174), is absolutely clear from the context.

$$m_j = m_l + m_s. \tag{5.180}$$

Hence the common eigenstates of the operators of this group are fully defined by just four quantum numbers, for example, l , m_l , s , and m_s . For some calculations, especially those for the systems whose Hamiltonians include only the operators of this group, it is convenient to use this set of eigenstates as the basis; frequently this approach is called the *uncoupled representation*. The most important example of such a situation is a non-relativistic particle moving in a spherically-symmetric potential (3.155), whose Hamiltonian does not depend on its spin. As we have seen in the previous section, its stationary states correspond to definite l and m_l .

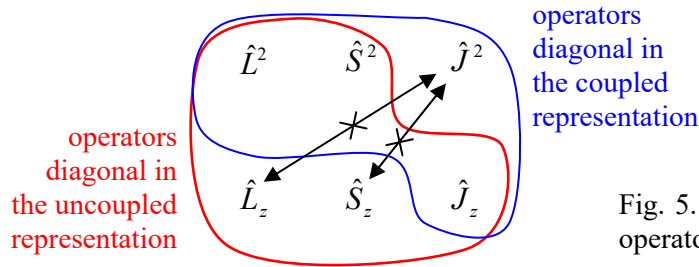


Fig. 5.12. The Venn diagram of angular momentum operators, and their mutually-commuting groups.

However, in some situations, interactions between the orbital and spin degrees of freedom (in the common jargon, the *spin-orbit coupling*) cannot be ignored; this interaction leads in particular to splitting (called the *fine structure*) of the atomic energy levels even in the absence of external magnetic field. I will discuss these effects in detail in the next chapter and now will only note that they may be described by a term proportional to the product $\hat{\mathbf{L}} \cdot \hat{\mathbf{S}}$ in the particle's Hamiltonian. If this term is substantial, the uncoupled representation becomes inconvenient. Indeed, writing

$$\hat{J}^2 = (\hat{\mathbf{L}} + \hat{\mathbf{S}})^2 = \hat{L}^2 + \hat{S}^2 + 2\hat{\mathbf{L}} \cdot \hat{\mathbf{S}}, \quad \text{so that } 2\hat{\mathbf{L}} \cdot \hat{\mathbf{S}} = \hat{J}^2 - \hat{L}^2 - \hat{S}^2, \tag{5.181}$$

and looking at Fig. 12 again, we see that the operator $\hat{\mathbf{L}} \cdot \hat{\mathbf{S}}$ describing the spin-orbit coupling does not commute with operators \hat{L}_z and \hat{S}_z . This means that stationary states of the system with such a term in the Hamiltonian do not belong to the uncoupled representation's basis. On the other hand, Eq. (181) shows that the operator $\hat{\mathbf{L}} \cdot \hat{\mathbf{S}}$ does commute with all four operators of another group, encircled blue in Fig. 12. According to Eqs. (178), (179), and (181), all operators of that group also commute with each other, so they have a group of common eigenstates, described by the quantum numbers l , s , j , and m_j . This group is the basis for the so-called *coupled representation* of particle states.

Excluding, for the notation brevity, the quantum numbers l and s that are common for both groups, it is convenient to denote the common ket-vectors of each group as, respectively,

$$\begin{aligned} &|m_l, m_s\rangle, \quad \text{for the uncoupled representation's basis,} \\ &|j, m_j\rangle, \quad \text{for the coupled representation's basis.} \end{aligned} \tag{5.182}$$

Coupled and uncoupled bases

As we will see in the next chapter, for the solution of some important problems (e.g., the fine structure of atomic spectra and the Zeeman effect), we will need the relation between the kets $|j, m_j\rangle$ and the kets $|m_l, m_s\rangle$. This relation may be represented as the usual linear superposition,

$$|j, m_j\rangle = \sum_{m_l, m_s} |m_l, m_s\rangle \langle m_l, m_s | j, m_j\rangle. \quad (5.183)$$

The short brackets in this relation, essentially the elements of the unitary matrix of the transformation between two eigenstate bases (182), are called the *Clebsch-Gordan coefficients*.

The best (though imperfect) classical interpretation of Eq. (183) I can offer is as follows. If the lengths of the vectors \mathbf{L} and \mathbf{S} (in quantum mechanics associated with the numbers l and s , respectively), and also their scalar product $\mathbf{L}\cdot\mathbf{S}$, are all fixed, then so is the length of the vector $\mathbf{J} = \mathbf{L} + \mathbf{S}$ – whose length in quantum mechanics is described by the number j . Hence, the classical image of a specific eigenket $|j, m_j\rangle$, in which l, s, j , and m_j are all fixed, is a state in which L^2, S^2, J^2 , and J_z are fixed. However, this fixation still allows for an arbitrary rotation of the pair of vectors \mathbf{L} and \mathbf{S} (with a fixed angle between them, and hence fixed $\mathbf{L}\cdot\mathbf{S}$ and J^2) about the direction of the vector \mathbf{J} – see Fig. 13.

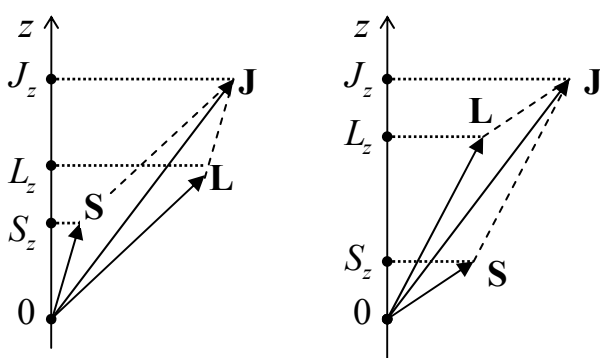


Fig. 5.13. A classical image of two different quantum states with the same quantum numbers l, s, j , and m_j , but different m_l and m_s .

Hence the components L_z and S_z in these conditions are *not* fixed, and in classical mechanics may take a continuum of values, two of which (with the largest and the smallest possible values of S_z) are shown in Fig. 13. In quantum mechanics, these components are quantized, with their states represented by eigenkets $|m_l, m_s\rangle$, so a linear combination of such kets is necessary to represent every ket $|j, m_j\rangle$. This is exactly what Eq. (183) does.

Some properties of the Clebsch-Gordan coefficients $\langle m_l, m_s | j, m_j\rangle$ may be readily established. For example, the coefficients do not vanish only if the involved magnetic quantum numbers satisfy Eq. (180). In our current case, this relation is not an elementary corollary of Eq. (171), because the Clebsch-Gordan coefficients, with the quantum numbers m_l, m_s in one state vector, and m_j in the other state vector, characterize the relationship between different groups of the basis states, so we need to prove this fact; let us do that. All matrix elements of the null-operator

$$\hat{J}_z - (\hat{L}_z + \hat{S}_z) = \hat{0} \quad (5.184)$$

should equal zero in any basis; in particular

$$\langle j, m_j | \hat{J}_z - (\hat{L}_z + \hat{S}_z) | m_l, m_s \rangle = 0. \quad (5.185)$$

Acting by the operator \hat{J}_z upon the bra-vector, and by the sum $(\hat{L}_z + \hat{S}_z)$ upon the ket-vector, we get

$$[m_j - (m_l + m_s)] \langle j, m_j | m_l, m_s \rangle = 0, \quad (5.186)$$

thus proving that

$$\langle m_l, m_s | j, m_s \rangle \equiv \langle j, m_s | m_l, m_s \rangle^* = 0, \quad \text{if } m_j \neq m_l + m_s. \quad (5.187)$$

As we will see in a minute, this property will enable us, in particular, to establish the range of possible values of the quantum number j , at fixed l and s .

For the most important case of spin- $\frac{1}{2}$ particles (with $s = \frac{1}{2}$, and hence $m_s = \pm \frac{1}{2}$), whose uncoupled representation basis includes $2 \times (2l + 1)$ states, the restriction (187) enables the representation of all non-zero Clebsch-Gordan coefficients on the simple “rectangular” diagram shown in Fig. 14. Indeed, each coupled-representation eigenket $|j, m_j\rangle$, with $m_j = m_l + m_s = m_l \pm \frac{1}{2}$, may be related by non-zero Clebsch-Gordan coefficients to at most two uncoupled-representation eigenstates $|m_l, m_s\rangle$. Since m_l may only take integer values from $-l$ to $+l$, m_j may only take semi-integer values on the interval $[-l - \frac{1}{2}, l + \frac{1}{2}]$. Hence, by the definition of j as $(m_j)_{\max}$, its maximum value has to be $l + \frac{1}{2}$, and for $m_j = l + \frac{1}{2}$, this is the only possible value with this j . This means that the uncoupled state with $m_l = l$ and $m_s = \frac{1}{2}$ should be identical to the coupled-representation state with $j = l + \frac{1}{2}$ and $m_j = l + \frac{1}{2}$:

$$|j = l + \frac{1}{2}, m_j = l + \frac{1}{2}\rangle = |m_l = m_j - \frac{1}{2}, m_s = +\frac{1}{2}\rangle. \quad (5.188)$$

In Fig. 14, these two identical states are represented by the top-rightmost point (the uncoupled representation) and the sloped line passing through it (the coupled representation).

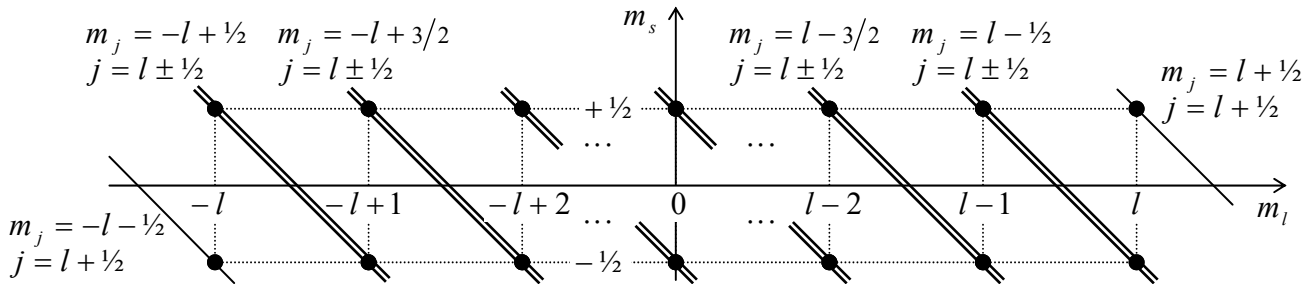


Fig. 5.14. A graphical representation of possible basis states of a spin- $\frac{1}{2}$ particle with a fixed l . Each dot corresponds to an uncoupled-representation ket-vector $|m_l, m_s\rangle$, while each sloped line corresponds to one coupled-representation ket-vector $|j, m_j\rangle$, related by Eq. (183) to the kets $|m_l, m_s\rangle$ whose dots it connects.

However, already the next value of this quantum number, $m_j = l - \frac{1}{2}$, is compatible with two values of j , so each $|m_l, m_s\rangle$ ket has to be related to two $|j, m_j\rangle$ kets by two Clebsch-Gordan coefficients. Since j changes in unit steps, these values of j have to be $l \pm \frac{1}{2}$. This choice,

$$j = l \pm \frac{1}{2}, \quad (5.189)$$

where the alternating sign is independent of the sign of m_s , evidently satisfies all lower values of m_j as well – see Fig. 14.⁵⁰ (Again, only one value, $j = l + \frac{1}{2}$, is necessary to represent the state with the lowest $m_j = -l - \frac{1}{2}$ – see the bottom-leftmost point of that diagram.)

⁵⁰ Eq. (189) may be readily generalized to the case of arbitrary spin s : j may only take values that differ by 1, within the interval $[|l - s|, l + s]$. This important result (whose proof is left for the reader’s exercise) allows a semi-quantitative classical interpretation in terms of the vector diagrams shown in Fig. 13: in them, the largest value of j corresponds to the parallel alignment of the vectors \mathbf{L} and \mathbf{S} , while its smallest value, to their antiparallel alignment.

Note that the total number of the coupled-representation states is $1 + 2 \times 2l + 1 \equiv 2(2l + 1)$, i.e. is the same as those in the uncoupled representation. So, for spin- $\frac{1}{2}$ systems, each sum (183), for fixed j and m_j (plus the fixed common parameter l , plus the common $s = \frac{1}{2}$), has at most two terms, i.e. involves at most two Clebsch-Gordan coefficients.

These coefficients may be calculated in a few steps, all but the last one rather simple even for arbitrary spin s . First, the similarity of the vector operators $\hat{\mathbf{J}}$ and $\hat{\mathbf{S}}$ to the operator $\hat{\mathbf{L}}$, expressed by Eqs. (169), (175), and (177), may be used to argue that the matrix elements of the operators \hat{S}_{\pm} and \hat{J}_{\pm} , defined similarly to \hat{L}_{\pm} , have the matrix elements similar to those given by Eq. (164). Next, acting by the operator $\hat{J}_{\pm} = \hat{L}_{\pm} + \hat{S}_{\pm}$ upon both parts of Eq. (183), and then inner-multiplying the result by the bra vector $\langle m_l, m_s |$ and using the above matrix elements, we may get recurrence relations for the Clebsch-Gordan coefficients with adjacent values of m_l , m_s , and m_j . Finally, these relations may be sequentially applied to the adjacent states in both representations, starting from any of the two states common for them – for example, from the state with the ket-vector (188), corresponding to the top-rightmost point in Fig. 14.

Let me leave these straightforward but a bit tedious calculations for the reader's exercise, and just quote the final result of this procedure for $s = \frac{1}{2}$:⁵¹

$$\begin{aligned} \langle m_l = m_j - \frac{1}{2}, m_s = +\frac{1}{2} | j = l \pm \frac{1}{2}, m_j \rangle &= \pm \left(\frac{l \pm m_j + \frac{1}{2}}{2l + 1} \right)^{1/2}, \\ \langle m_l = m_j + \frac{1}{2}, m_s = -\frac{1}{2} | j = l \pm \frac{1}{2}, m_j \rangle &= + \left(\frac{l \mp m_j + \frac{1}{2}}{2l + 1} \right)^{1/2}. \end{aligned} \quad (5.190)$$

Clebsch –
Gordan
coefficients
for $s = \frac{1}{2}$

As a simple example, let an electron be in the p -state ($l = 1$) with definite $j = \frac{1}{2}$ and $m_j = \frac{1}{2}$, and we want to know the probability of its spin being directed down ($m_s = -\frac{1}{2}$). Since in this case, $j = l - \frac{1}{2}$, the above formulas should be used with the upper signs, giving

$$\begin{aligned} \langle m_l = 0, m_s = +\frac{1}{2} | j = \frac{1}{2}, m_j = \frac{1}{2} \rangle &= - \left(\frac{1 - \frac{1}{2} + \frac{1}{2}}{2 \cdot 1 + 1} \right)^{1/2} \equiv - \left(\frac{1}{3} \right)^{1/2}, \\ \langle m_l = 1, m_s = -\frac{1}{2} | j = \frac{1}{2}, m_j = \frac{1}{2} \rangle &= + \left(\frac{1 + \frac{1}{2} + \frac{1}{2}}{2l + 1} \right)^{1/2} \equiv + \left(\frac{2}{3} \right)^{1/2}, \end{aligned} \quad (5.191)$$

so the general Eq. (183) takes the form

$$| j = \frac{1}{2}, m_j = \frac{1}{2} \rangle = - \left(\frac{1}{3} \right)^{1/2} | m_l = 0, m_s = +\frac{1}{2} \rangle + \left(\frac{2}{3} \right)^{1/2} | m_l = 1, m_s = -\frac{1}{2} \rangle, \quad (5.192)$$

and the probability of the spin-down state with $m_s = -\frac{1}{2}$ is $W_{\downarrow} = 2/3$.

In this course, Eqs. (190) will be used mostly in Sec. 6.4 for an analysis of the anomalous Zeeman effect. Also, the angular momentum addition rules described above are also valid for the addition of angular momenta of multiparticle system components, so we will revisit them in Chapter 8.

⁵¹ For arbitrary spin s , the calculations and even the final expressions for the Clebsch-Gordan coefficients are rather bulky. They may be found, typically in a table form, mostly in special monographs – see, e.g., A. Edmonds, *Angular Momentum in Quantum Mechanics*, Princeton U. Press, 1957.

To conclude this section, I have to note that the Clebsch-Gordan coefficients (for arbitrary s) participate also in the so-called *Wigner-Eckart theorem* that expresses the matrix elements of *spherical tensor operators*, in the coupled-representation basis $|j, m_j\rangle$, via a reduced set of matrix elements. This theorem may be useful, for example, for the calculation of the rate of quantum transitions to/from high- n states in spherically symmetric potentials. Unfortunately, a discussion of this theorem and its applications would require a higher mathematical background than I can expect from my readers and more time/space than I can afford.⁵²

5.8. Exercise problems

5.1. Use the discussion in Sec. 1 to find an alternative solution of Problem 4.18.

5.2. A spin- $1/2$ with a gyromagnetic ratio γ is placed into an external magnetic field, with a time-independent orientation, its magnitude $\mathcal{B}(t)$ being an arbitrary function of time. Find explicit expressions for the Heisenberg operators and the expectation values of all three Cartesian components of the spin as functions of time, in a coordinate system of your choice.

5.3. A two-level system is in the quantum state α described by the ket-vector $|\alpha\rangle = \alpha_\uparrow|\uparrow\rangle + \alpha_\downarrow|\downarrow\rangle$, with given (generally, complex) c -number coefficients $\alpha_{\uparrow\downarrow}$. Prove that we can always select such a geometric c -number vector $\mathbf{c} = \{c_x, c_y, c_z\}$ that α would be an eigenstate of $\mathbf{c} \cdot \hat{\boldsymbol{\sigma}}$, where $\hat{\boldsymbol{\sigma}}$ is the Pauli vector operator. Find all possible values of \mathbf{c} satisfying this condition, and the second eigenstate (orthogonal to α) of the operator $\mathbf{c} \cdot \hat{\boldsymbol{\sigma}}$. Give a Bloch-sphere interpretation of your result.

5.4. Rewrite the key formulas of the solutions of Problems 4.27-4.29 in terms of the Bloch sphere angles, and verify at least one of them using the general relations of Sec. 5.1 of the lecture notes.

5.5. A spin- $1/2$ with a gyromagnetic ratio $\gamma > 0$ was placed into a time-independent magnetic field $\mathcal{B}_0 = \mathcal{B}_0 \mathbf{n}_z$ and let relax into the lowest-energy state. At $t = 0$, an additional field $\mathcal{B}_1(t)$ is turned on; its vector has a constant magnitude but rotates within the $[x, y]$ -plane with an angular velocity ω . Calculate the expectation values of all Cartesian components of the spin at $t \geq 0$, and discuss the representation of its dynamics on the Bloch sphere.

5.6.* Analyze statistics of the spacing $S \equiv E_+ - E_-$ between energy levels of a two-level system, assuming that all elements $H_{jj'}$ of its Hamiltonian matrix (2) are independent random numbers, with equal and constant probability densities within the energy interval of interest. Compare the result with that for a purely diagonal Hamiltonian matrix, with a similar probability distribution of its random diagonal elements.

5.7. For a periodic motion of a single particle in a confining potential $U(\mathbf{r})$, the *virial theorem* of non-relativistic classical mechanics⁵³ is reduced to the following equality:

⁵² For the interested reader, I can recommend either Sec. 17.7 in E. Merzbacher, *Quantum Mechanics*, 3rd ed., Wiley, 1998, or Sec. 3.10 in J. Sakurai, *Modern Quantum Mechanics*, Addison-Wesley, 1994.

⁵³ See, e.g., CM Problem 1.12.

$$\bar{T} = \frac{1}{2} \overline{\mathbf{r} \cdot \nabla U},$$

where T is the particle's kinetic energy, and the top bar means averaging over the time period of motion. Prove the following quantum-mechanical version of the theorem for an arbitrary stationary state, in the absence of spin effects:

$$\langle T \rangle = \frac{1}{2} \langle \mathbf{r} \cdot \nabla U \rangle,$$

where the angular brackets denote (as usual in this course) the expectation values of the observables.

Hint: Mimicking the proof of the classical virial theorem, consider the time evolution of the following operator: $\hat{G} \equiv \hat{\mathbf{r}} \cdot \hat{\mathbf{p}}$.

5.8. A non-relativistic 1D particle moves in the spherically symmetric potential $U(r) = C \ln(r/R)$. Prove that for:

- (i) $\langle v^2 \rangle$ is the same in each eigenstate, and
- (ii) the spacing between the energy levels is independent of the particle's mass.

5.9. Calculate, in the WKB approximation, the transparency \mathcal{T} of the following saddle-shaped potential barrier:

$$U(x, y) = U_0 \left(1 + \frac{xy}{a^2} \right),$$

where $U_0 > 0$ and a are real constants, for tunneling of a 2D particle with energy $E < U_0$.

5.10. In the WKB approximation, calculate the so-called *Gamow factor*⁵⁴ for the alpha decay of atomic nuclei, i.e. the exponential factor in the transparency of the potential barrier resulting from the following simple model for the alpha-particle's potential energy as a function of its distance from the nuclear center:

$$U(r) = \begin{cases} U_0 < 0, & \text{for } r < R, \\ \frac{ZZ'e^2}{4\pi\epsilon_0 r}, & \text{for } R < r, \end{cases}$$

where $Ze = 2e > 0$ is the charge of the particle, $Z'e > 0$ is that of the nucleus after the decay, and R is the nucleus' radius.

5.11. Use the WKB approximation to calculate the average time of ionization of a hydrogen atom, initially in its ground state, made metastable by the application of an additional weak, uniform, time-independent electric field \mathcal{E} . Formulate the conditions of validity of your result.

5.12. For a 1D harmonic oscillator with mass m and frequency ω_0 , calculate:

- (i) all matrix elements $\langle n | \hat{x}^3 | n' \rangle$, and
- (ii) the diagonal matrix elements $\langle n | \hat{x}^4 | n \rangle$,

where n and n' are arbitrary Fock states.

⁵⁴ Named after G. Gamow, who made this calculation as early as in 1928.

5.13. Calculate the sum (over all $n > 0$) of the so-called *oscillator strengths*,

$$f_n \equiv \frac{2m}{\hbar^2} (E_n - E_0) |\langle n | \hat{x} | 0 \rangle|^2,$$

- (i) for a 1D harmonic oscillator, and
 (ii) for a 1D particle confined in an arbitrary stationary potential.⁵⁵

5.14. Prove the so-called *Bethe sum rule*,

$$\sum_{n'} (E_{n'} - E_n) |\langle n | e^{ik\hat{x}} | n' \rangle|^2 = \frac{\hbar^2 k^2}{2m}$$

(where k is any c -number constant), valid for a 1D particle moving in an arbitrary time-independent potential $U(x)$, and discuss its relation with the Thomas-Reiche-Kuhn sum rule whose derivation was the subject of the previous problem.

Hint: Calculate the expectation value, in a stationary state n , of the double commutator

$$\hat{D} \equiv \left[\left[\hat{H}, e^{ik\hat{x}} \right], e^{-ik\hat{x}} \right]$$

in two ways: first, just by spelling out both commutators, and, second, by using the commutation relations between operators \hat{p}_x and $e^{ik\hat{x}}$, and compare the results.

5.15. Spell out the commutator $\left[\hat{a}, \exp\{\lambda \hat{a}^\dagger\} \right]$, where \hat{a}^\dagger and \hat{a} are the creation-annihilation operators (5.65), and λ is a c -number.

5.16. Given Eq. (116), prove Eq. (117) by using the hint given in the accompanying note.

5.17. Use Eqs. (116)-(117) to simplify the following operators:

- (i) $\exp\{+ia\hat{x}\} \hat{p}_x \exp\{-ia\hat{x}\}$, and
 (ii) $\exp\{+ia\hat{p}_x\} \hat{x} \exp\{-ia\hat{p}_x\}$,

where a is a c -number.

5.18.* Derive the commutation relation between the number operator (5.73) and a reasonably defined quantum-mechanical operator describing the harmonic oscillator's phase φ . Obtain the uncertainty relation for the corresponding observables, and explore its limit at $N \gg 1$.

5.19. At $t = 0$, a 1D harmonic oscillator was in a state described by the ket-vector

$$|\alpha\rangle = \frac{1}{\sqrt{2}} (|31\rangle + |32\rangle),$$

where $|n\rangle$ are the ket-vectors of the stationary (Fock) states of the oscillator. Calculate:

- (i) the expectation value of the oscillator's energy, and

⁵⁵ This *Thomas-Reiche-Kuhn sum rule* is important for applications because the coefficients f_n describe, in particular, the intensity of dipole quantum transitions between the n^{th} energy level and the ground state – see, e.g., Sec. 9.2 and also EM Sec. 7.2.

(ii) the time evolution of the expectation values of its coordinate and momentum.

5.20.* Re-derive the London dispersion force's potential of the interaction of two isotropic 3D harmonic oscillators (already calculated in Problem 3.20), using the language of mutually-induced polarization.

5.21. An external force pulse $F(t)$, of a finite time duration \mathcal{T} , is exerted on a 1D harmonic oscillator, initially in its ground state. Use the Heisenberg-picture equations of motion to calculate:

- (i) the expectation values of the oscillator's coordinate and momentum and their uncertainties, at an arbitrary moment,
- (ii) its total energy after the end of the pulse.

5.22. Use Eqs. (144)-(145) to calculate the uncertainties δx and δp for a harmonic oscillator in its squeezed ground state, and in particular, to prove Eqs. (143) for the case $\theta = 0$.

5.23. Calculate the energy of a harmonic oscillator in the squeezed ground state ζ .

5.24.* Prove that the squeezed ground state described by Eqs. (142) and (144)-(145) may be sustained by a sinusoidal modulation of a harmonic oscillator's parameter, and calculate the squeezing factor r as a function of the parameter modulation depth, assuming that the depth is small and the oscillator's damping is negligible.

5.25. Use Eqs. (148) to prove that at negligible spin effects, the operators \hat{L}_j and \hat{L}^2 commute with the Hamiltonian of a particle placed in any central potential field.

5.26. Use Eqs. (149)-(150) and (153) to prove Eqs. (155).

5.27. Derive Eq. (164) by using any of the prior formulas.

5.28. Derive the expression $\langle L^2 \rangle = \hbar^2 l(l+1)$ from basic statistics, by assuming that all $(2l+1)$ values $L_z = \hbar m$ of a system with a fixed integer number l have equal probability, and that the system is isotropic. Explain why this statistical picture cannot be used for proof of Eq. (5.163).

5.29. In the basis of common eigenstates of the operators \hat{L}_z and \hat{L}^2 , described by kets $|l, m\rangle$:

- (i) calculate the matrix elements $\langle l, m_1 | \hat{L}_x | l, m_2 \rangle$ and $\langle l, m_1 | \hat{L}_x^2 | l, m_2 \rangle$,
- (ii) spell out your results for diagonal matrix elements (with $m_1 = m_2$) and their y -axis counterparts, and
- (iii) calculate the diagonal matrix elements $\langle l, m | \hat{L}_x \hat{L}_y | l, m \rangle$ and $\langle l, m | \hat{L}_y \hat{L}_x | l, m \rangle$.

5.30. For the state described by the common eigenket $|l, m\rangle$ of the operators \hat{L}_z and \hat{L}^2 in a reference frame $\{x, y, z\}$, calculate the expectation values $\langle L_z \rangle$ and $\langle L_z'^2 \rangle$ in the reference frame whose z' -axis forms angle θ with the z -axis.

5.31. Write down the matrices of the following angular momentum operators: \hat{L}_x , \hat{L}_y , \hat{L}_z , and \hat{L}_\pm , in the z -basis of the $\{l, m\}$ states with $l = 1$.

5.32. Calculate the angular factor of the orbital wavefunction of a particle with a definite value of L^2 , equal to $6\hbar^2$, and the largest possible value of L_x . What is this value?

5.33. For the state with the wavefunction $\psi = Cxye^{-\lambda r}$, with a real positive λ , calculate:

- (i) the expectation values of the observables L_x , L_y , L_z , and L^2 , and
- (ii) the normalization constant C .

5.34. An angular state of a spinless particle is described by the following ket-vector:

$$|\alpha\rangle = \frac{1}{\sqrt{2}}(|l=3, m=0\rangle + |l=3, m=1\rangle).$$

Calculate the expectation values of the x - and y -components of its angular momentum. Is the result sensitive to a possible phase shift between the component eigenkets?

5.35. A particle is in a quantum state α with the orbital wavefunction proportional to the spherical harmonic $Y_1^1(\theta, \varphi)$. Find the angular dependence of the wavefunctions corresponding to the following ket-vectors:

$$(i) \hat{L}_x|\alpha\rangle, \quad (ii) \hat{L}_y|\alpha\rangle, \quad (iii) \hat{L}_z|\alpha\rangle, \quad (iv) \hat{L}_+\hat{L}_-|\alpha\rangle, \quad \text{and} \quad (v) \hat{L}^2|\alpha\rangle.$$

5.36. A charged, spinless 2D particle of mass m is trapped in the potential well $U(x, y) = m\omega_0^2(x^2 + y^2)/2$. Calculate its energy spectrum in the presence of a uniform magnetic field \mathcal{B} normal to the $[x, y]$ -plane of the particle's motion.

5.37. Solve the previous problem for a spinless 3D particle, placed (in addition to a uniform magnetic field \mathcal{B}) into a spherically-symmetric potential well $U(\mathbf{r}) = m\omega_0^2 r^2/2$.

5.38. Calculate the spectrum of rotational energies of an axially symmetric rigid macroscopic body.

5.39. Simplify the double commutator $[\hat{r}_j, [\hat{L}^2, \hat{r}_j]]$.

5.40. Prove the following commutation relation:

$$[\hat{L}^2, [\hat{L}^2, \hat{r}_j]] = 2\hbar^2(\hat{r}_j\hat{L}^2 + \hat{L}^2\hat{r}_j).$$

5.41. Use the commutation relation proved in the previous problem and Eq. (148) to prove the orbital electric-dipole transition selection rules mentioned in Sec. 6.

5.42. Express the commutators listed in Eq. (179), $[\hat{J}^2, \hat{L}_z]$ and $[\hat{J}^2, \hat{S}_z]$, via \hat{L}_j and \hat{S}_j .

5.43. Find the operator $\hat{\mathcal{T}}_\phi$ describing a quantum state's rotation by angle ϕ about a certain axis, by using the similarity of this operation with the shift of a Cartesian coordinate, discussed in Sec. 5. Then use this operator to calculate the probabilities of measurements of spin- $1/2$ components of particles with z -polarized spin, by a Stern-Gerlach instrument turned by angle θ within the $[z, x]$ plane, where y is the axis of particle propagation – see Fig. 4.1.⁵⁶

5.44. The rotation operator $\hat{\mathcal{T}}_\phi$ analyzed in the previous problem and the linear translation operator $\hat{\mathcal{T}}_\lambda$ discussed in Sec. 5 have a similar structure:

$$\hat{\mathcal{T}}_\lambda = \exp\{-i\hat{C}\lambda/\hbar\},$$

where λ is a real c -number scaling the shift and \hat{C} is a Hermitian operator that does not explicitly depend on time.

(i) Prove that such operators are unitary.

(ii) Prove that if the shift by λ , induced by the operator $\hat{\mathcal{T}}_\lambda$, leaves the Hamiltonian of some system unchanged for any λ , then $\langle C \rangle$ is a constant of motion for any initial state of the system.

(iii) Discuss what the last conclusion means for the particular operators $\hat{\mathcal{T}}_x$ and $\hat{\mathcal{T}}_\phi$.

5.45. A particle with spin s is in a state with definite quantum numbers l and j . Prove that the observable $\mathbf{L}\cdot\mathbf{S}$ also has a definite value and calculate it.

5.46. For a spin- $1/2$ particle in a state with definite quantum numbers l , m_l , and m_s , calculate the expectation value of the observable \mathcal{J}^2 and the probabilities of all its possible values. Interpret your results in terms of the Clebsch-Gordan coefficients (190).

5.47. Derive general recurrence relations for the Clebsch-Gordan coefficients for a particle with spin s .

Hint: By using the similarity of the commutation relations discussed in Sec. 7, write the relations similar to Eqs. (164) for other components of the angular momentum, and then apply them to Eq. (170).

5.48. Use the recurrence relations derived in the previous problem to prove Eqs. (190) for the spin- $1/2$ Clebsch-Gordan coefficients.

5.49. A spin- $1/2$ particle is in a state with definite values of L^2 , \mathcal{J}^2 , and J_z . Find all possible values of the observables S^2 , S_z , and L_z , the probability of each listed value, and the expectation value for each of these observables.

5.50. Re-solve the Landau-level problem discussed in Sec. 3.2, now for a spin- $1/2$ particle. Discuss the result for the particular case of an electron.

⁵⁶ Note that the last task is just a particular case of Problem 4.18 (see also Problem 1).

5.51. In the Heisenberg picture of quantum dynamics, find an explicit relation between the operators of velocity $\hat{\mathbf{v}} \equiv d\hat{\mathbf{r}}/dt$ and acceleration $\hat{\mathbf{a}} \equiv d\hat{\mathbf{v}}/dt$ of a nonrelativistic particle with an electric charge q , moving in an arbitrary external electromagnetic field. Compare the result with the corresponding classical expression.

Hint: For the orbital motion's description, you may use Eq. (3.26).

5.52. One byproduct of the solution of Problem 47 was the following relation for the spin operators (valid for any spin s):

$$\langle m_s \pm 1 | \hat{S}_{\pm} | m_s \rangle = \hbar [(s \pm m_s + 1)(s \mp m_s)]^{1/2}.$$

Use this result to spell out the matrices S_x , S_y , S_z , and S^2 of a particle with $s = 1$, in the z -basis – defined as the basis in which the matrix S_z is diagonal.

5.53.* For a particle with an arbitrary spin s , find the ranges of the quantum numbers m_j and j that are necessary to describe, in the coupled-representation basis:

- (i) all states with a definite quantum number l , and
- (ii) a state with definite values of not only l but also m_l and m_s .

Give an interpretation of your results in terms of the classical vector diagram – see, e.g., Fig. 13.

5.54. For a particle with spin s , find the range of the quantum numbers j necessary to describe, in the coupled-representation basis, all states with definite quantum numbers l and m_l .

5.55. A particle of mass m , with electric charge q and spin s , free to move along a planar circle of a radius R , is placed into a constant uniform magnetic field \mathcal{B} directed normally to the circle's plane. Calculate the energy spectrum of the system. Explore and interpret the particular form the result takes when the particle is an electron with the g -factor $g_e \approx 2$.